AAPM TG 191: Clinical use of luminescent dosimeters: TLDs and OSLDs

Stephen F. Kry[a)], and Paola Alvarez
The University of Texas MD Anderson Cancer Center, Houston, TX, USA

Joanna E. Cygler
The Ottawa Hospital Cancer Center, Ottawa, ON, USA

Larry A. DeWerd
University of Wisconsin – Madison, Madison, WI, USA

Rebecca M. Howell
The University of Texas MD Anderson Cancer Center, Houston, TX, USA

Sanford Meeks
University of Florida Health Cancer Center, Orlando, FL, USA

Jennifer O'Daniel
Duke University Medical Center, Durham, NC, USA

Chester Reft
University of Chicago, Chicago, IL, USA

Gabriel Sawakuchi
The University of Texas MD Anderson Cancer Center, Houston, TX, USA

Eduardo G. Yukihara
Paul Scherrer Institut, Geneva, Switzerland

Dimitris Mihailidis
University of Pennsylvania, Philadelphia, PA, USA

(Received 10 June 2019; revised 27 August 2019; accepted for publication 28 August 2019; published 6 December 2019)

Thermoluminescent dosimeters (TLD) and optically stimulated luminescent dosimeters (OSLD) are practical, accurate, and precise tools for point dosimetry in medical physics applications. The charges of Task Group 191 were to detail the methodologies for practical and optimal luminescence dosimetry in a clinical setting. This includes: (a) to review the variety of TLD/OSLD materials available, including features and limitations of each; (b) to outline the optimal steps to achieve accurate and precise dosimetry with luminescent detectors and to evaluate the uncertainty induced when less rigorous procedures are used; (c) to develop consensus guidelines on the optimal use of luminescent dosimeters for clinical practice; and (d) to develop guidelines for special medically relevant uses of TLDs/OSLDs such as mixed photon/neutron field dosimetry, particle beam dosimetry, and skin dosimetry. While this report provides general guidelines for TLD and OSLD processes, the report provides specific details for TLD-100 and nanoDot™ dosimeters because of their prevalence in clinical practice. [https://doi.org/10.1002/mp.13839]

Key words: dosimetry, luminescence, OSLD, Task Group, TLD

TABLE OF CONTENTS

1. INTRODUCTION

1.A. Purpose and scope

Luminescence dosimetry is the measurement of absorbed dose from ionizing radiation based on the emission of visible photons by a phosphor. Luminescence dosimetry may refer to thermoluminescence (TL), optically stimulated luminescence (OSL), or other types of photon emission processes including radiophotoluminescence, radioluminescence, and scintillation. This task group focuses on the passive use (i.e., readout of the phosphor subsequent to irradiation) of thermoluminescence dosimeters (TLD) and optically stimulated luminescence dosimeters (OSLD), herein referred to as luminescent dosimeters (LDs), in a medical environment. This report focuses primarily on those dosimeters most commonly used in clinical practice: LiF:Mg,Ti (i.e., TLD-100, Thermo Fischer Scientific, Waltham MA) and Al_2O_3:C dosimeters (i.e., nanoDot^{TM}, Landauer Inc., Glenwood Il). These dosimeters have been used extensively because of their small size, precision, availability, reusability, and other favorable dosimetric characteristics. However, luminescence dosimetry can be performed with many different materials, several of which are discussed in chapter 3.

The charges of this task group were to (a) review the variety of TLD/OSLD materials, (b) outline optimal steps to achieve accurate and precise dosimetry, including uncertainty analysis, (c) develop consensus guidelines on the optimal use of luminescent dosimeters in clinical practice, and (d) develop guidelines for special medically relevant uses of TLD and OSLD. To achieve these, this report addresses correction factors, handling, and processing issues necessary for precise dosimetry, along with the dose measurement formalisms (chapters 4–6). Examples of correction factors for TLD-100 and nanoDot^{TM} dosimeters are shown throughout, but these are intended only to serve as examples of the magnitude of these correction factors. Actual correction factors may depend on the production batch of the crystal, manufacturer, and potentially on the reader. Furthermore, correction factors for other types of TLD/OSLD materials will often be very different. Therefore, the data presented herein serve only as a guide to the process, rather than as absolute values to be broadly applied. Additionally, there are published modifications to traditional LD use, such as high-dose preirradiation of OSLD.[1] This TG report focuses on the mainstream approach to LD use that has been thoroughly evaluated in the literature. Use of other approaches or modifications to the procedures described herein should be done with caution because these approaches are less well vetted.

This report focuses on the clinical applications of TLD and OSLD. Some sections, such as 2 and 3 on the theory of, and different types of LDs, are more general and only a brief overview is provided in this report. Particularly for sections such as these, more complete information is available in several comprehensive references on TL[2–7] and OSL,[8–13] and on solid state dosimetry.[14]

1.B. Definitions

Throughout the literature, a wide range of terms have been used to describe the same parameter in luminescent dosimetry. Here we provide suggested nomenclature consistent with American Association of Physicists in Medicine (AAPM) summer school reports.[9,15]

TLD	thermoluminescent dosimeter
OSLD	optically stimulated luminescent dosimeter
LD	luminescent dosimeter; the family of TLDs and OSLDs
Batch	a production run of LD crystal; unavoidable variations in impurity concentrations between batches affect sensitivity and other correction parameters
Element	a single detector from a batch

Standard	(italicized) an LD irradiated to a known dose to determine the dose response of the system; this is not a Primary Laboratory-derived quantity but is determined by the institution. The manner in which the institution determines the standard may result in tertiary or greater traceability
Experimental	(italicized) an LD irradiated as part of an experiment
Constancy Dosimeter	A *standard* OSLD used over many sessions (corrected for fading and depletion) used to verify the performance of the dosimetry system
Fading	spontaneous loss of signal with time
Depletion	partial loss of signal associated with the readout process (OSLD only)
M_{raw}	raw detector reading; counts or collected charge per unit mass
M_{corr}	the detector reading corrected for depletion, background, and element sensitivity as applicable
M_0	the detector reading of the *standard(s)*
D_0	the dose delivered to the *standard(s)*
N	system calibration coefficient, usually $N_{D,w}$ for dose to water; the inverse of the sensitivity of the system (i.e., system sensitivity)
k_Q	beam quality correction factor, including both intrinsic energy dependence and medium-dependent energy dependence
k_L	dose nonlinearity correction factor
k_F	signal fading correction factor
$k_{s,i}$	element sensitivity correction factor
k_d	depletion correction factor
k_θ	angular correction factor

2. THEORY

In a perfect crystalline insulator, the conduction and valence bands are separated by an energy difference of several eV, and there are no intermediate energy levels within this band gap. Luminescence detectors are created by adding impurities to these crystals, thereby introducing energy levels within the band gap in the vicinity of the impurities. During exposure to ionizing radiation [Fig. 1(a)], ionizations created within the detector material promote a number of electrons to the conduction band, leaving behind holes in the valence band. These electrons and holes can move in their respective energy bands until they recombine or are captured by defects (indicated by "electron trap" and "hole trap" in Fig. 1). In the absence of additional stimuli such as heating or illumination, these trapped charges can remain trapped for periods ranging from less than one second to thousands of years, depending primarily on the trap depth, that is, the energy difference between the trap level and the delocalized conduction or valence band.

During the readout process [Fig. 1(b)], stimulation by heat (TL) or light (OSL) releases the trapped charges. Once the trapped electron is released, it can recombine with the trapped hole, creating a defect in the excited state. TL or OSL results from the relaxation of these defects to return to the ground state by light emission. One should keep in mind that this model is simplified. Actual TL and OSL materials have many defects that may not give rise to observable TL/OSL signals but may act as competitors for the transitions represented in Fig. 1, causing changes in the TL/OSL properties. These competitors give rise to phenomena such as supralinearity of the dose response and sensitivity changes with detector's dose and annealing history.[16,17]

TL/OSL readers stimulate the detector, using either heat or light, and monitor the resultant luminescence with a photomultiplier tube (PMT), which converts the luminescence into "counts" or current. More detailed reviews of LD readers and readout processes are available in the literature.[8,13,16,18]

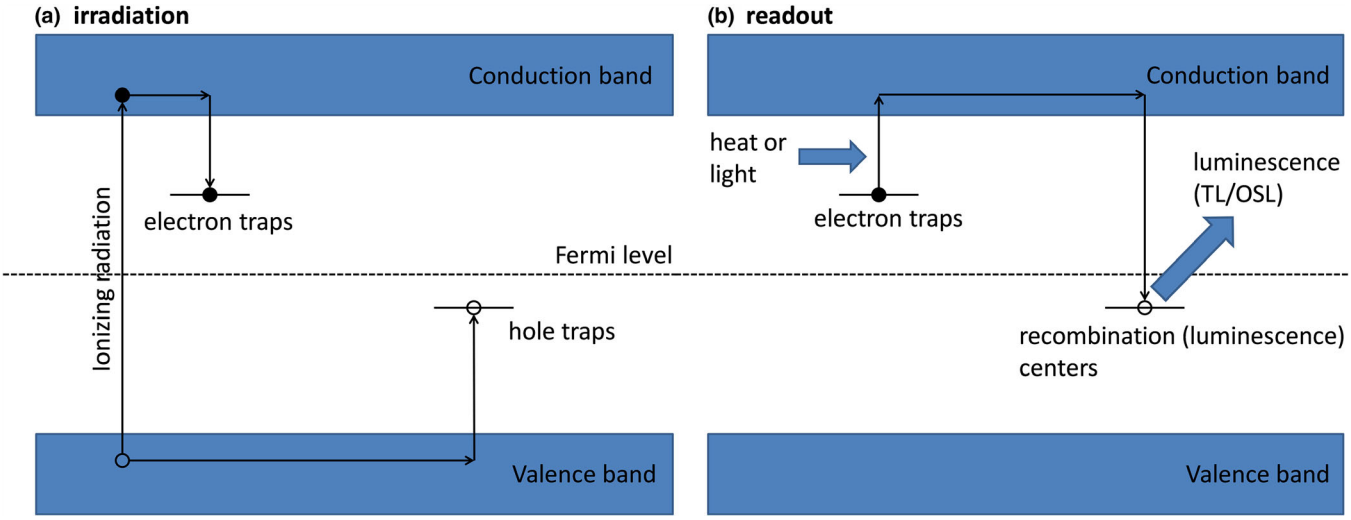

FIG. 1. Simplified energy level diagram representing the delocalized bands (valence band and conduction band) and the electronic transitions in Thermoluminescent/optically stimulated luminescent material during irradiation (a) and readout (b) where stimulation is provided by heat or light. In this illustration, the hole trap is more stable than the electron trap. Therefore, the electron trap is said to act as a trapping center, whereas the hole trap is said to act as a recombination center.

Thermoluminescent dosimeters are read by increasing the temperature of the detector while monitoring the TL emitted, either creating a glow curve graph of signal vs temperature or by recording the total signal for a portion of the heating process. In the former, the TL signal can be defined as the maximum intensity of a TL peak or the integrated TL intensity over a region of interest. Figure 2(a) illustrates a glow curve for LiF:Mg,Ti (TLD-100). Different trapping centers have different depths within the bandgap that require different temperatures for release. As the detector is heated, these trapping centers are stimulated sequentially, giving rise to a series of peaks. Both the temperature of the maximum peak and the maximum TL signal depend on the heating rate. To minimize the effect of heating rate fluctuations, the integral of the TL signal rather than its maximum is typically used to determine the dose. TL peaks with maxima around 200–225°C are best for dosimetry because of their stability at room temperature (Peak 5 in Fig. 2). TL peaks at lower temperatures are due to shallow trapping levels in the band gap and may be unstable at room temperature. TL peaks appearing at higher temperatures may suffer interference from infrared black-body radiation and spurious signals. These effects are mitigated by using a bandpass filter to eliminate the infrared signals and by flowing an inert gas such as N_2 or Ar over the TL phosphor during heating to reduce spurious signals. The relative importance of these peaks and the sensitivity of the detector will depend on annealing regimens before irradiation. Because the TL readout depletes the majority of the trapping centers, less than 1% of the original signal should be observed if the material is read again without irradiation.

While different peaks can include different information about the irradiation, in clinical practice the standard practice is to simply integrate the entire glow curve to yield the overall signal. To ensure reproducible results, a consistent heating cycle should be used.

Figure 3(a) presents a typical configuration for a TLD reader. The heating source can be an ohmically heated pan, preheated N_2 gas, or an infrared light source. A typical heating cycle consists of a rapid increase to a moderate temperature during which the signal, primarily from unstable traps, is not recorded, followed by a linear temperature increase during which the TL glow curve is measured (e.g., peak 5 in Fig. 2). The final step is heating the crystal to a high temperature to anneal the TLD, emptying the deep traps that were untouched at lower temperatures.

Optically stimulated luminescent dosimeters can be read using light, either of constant intensity (continuous-wave technique) or variable intensity (pulsed technique). The OSL signal will decrease exponentially as the trapping centers are emptied [Fig. 2(b), illustrating a continuous-wave readout]. In the case of practical OSL materials, the OSL curve is not a single exponential because there are also multiple trapping centers. Simplistically, the traps can be classified into three types: shallow-depth traps that are unstable at room temperature, medium-depth traps that may be released via exposure to light in the visible spectrum, and deep-depth traps that once filled are very difficult, if not impossible, to empty. The behavior and interplay of these different trap types affect fading, reuse, and readout of OSLDs. The OSL decay curve is also affected by the type of stimulation light (broadband vs monochromatic), its intensity, and its duration. Increasing the stimulation intensity increases the initial OSL signal, but signal decay occurs faster as a result. In practice, most commercial readers stimulate the detector for approximately 1 s so that only a fraction of the trapped charge is released. For a continuous-wave illumination, the total signal over that stimulation time is recorded. If a pulsed technique is used, the stimulation is comprised of a series of short pulses of light with readout done during the periods when the stimulation source is off. This approach provides a better signal-to-noise ratio, but does not substantially impact the practical use or precision of the system.[19]

The basic elements of an OSL reader are represented in Fig. 3(b), although a transmission orientation of the light source and detector may also be used. A light source such as a laser, light-emitting diode (LED), or broadband lamp is used for stimulation. Optical filters are typically used in front of the light source to select specific stimulation wavelengths

Reader

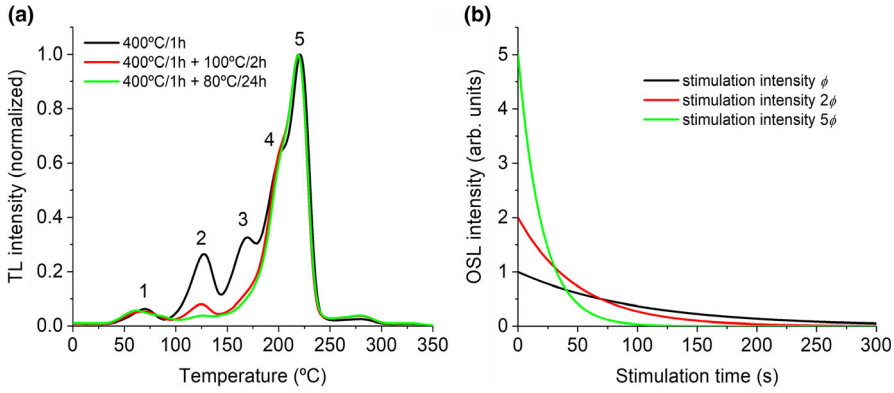

FIG. 2. (a) Thermoluminescent curves of LiF:Mg,Ti (TLD-100) subjected to different preirradiation annealing treatments. Peaks 1–5 correspond to different trapping centers (which yield signal at different temperatures); peak 5 occurs at the temperature of maximum signal. (b) optically stimulated luminescent curves that result from a hypothetical phosphor containing only one type of recombination center and only one type of optically active defect with a well-defined photoionization cross-section and illuminated with constant, monochromatic light with intensity ϕ, 2ϕ, or 5ϕ.

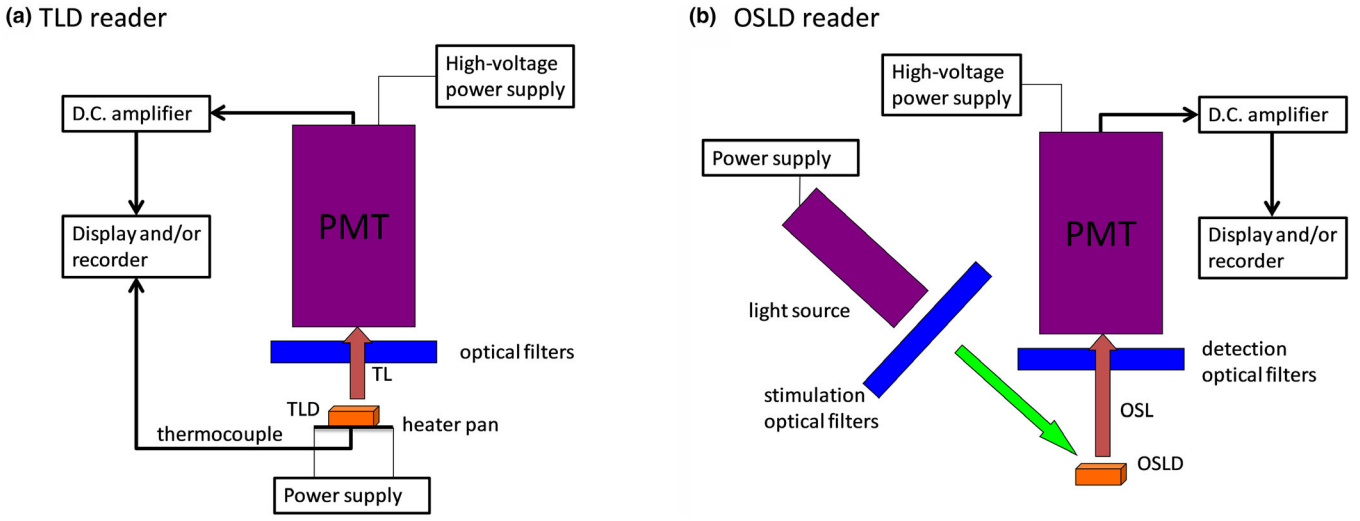

FIG. 3. Basic elements of (a) a thermoluminescent dosimeters reader and (b) an optically stimulated luminescent dosimeters reader.

and to block wavelengths that overlap with those of the OSL signal. Optical filters are also used in front of the PMT to block the stimulation light while transmitting the OSL signal. In the case of an Al_2O_3:C dosimeter, stimulation is typically performed using green light from a laser or LED (~525 nm), with the emission band in the blue (~420 nm).[20,21]

The dosimetric properties of a particular TL/OSL system depend on the entire dosimetry system, which includes the dosimeter, preparation procedure, dosimeter holder, reader, choice of signal, temperature rate and maximum, dose given, photomultiplier tube, and algorithm used to estimate the quantity of interest. Because they may influence the results, it is important to understand and be consistent in their use. To minimize the variations in system response, it is essential to have a stable, reproducible process of heating/illuminating the TLD/OSLD and a consistent light sensitivity of the PMT. This is aided by conducting a session-specific calibration of the detector as well as appropriate quality assurance procedures for the reader.

3. AVAILABLE DOSIMETRY SYSTEMS

3.A. Types of TLD/OSLD

Many materials exhibit luminescent properties that make them broadly applicable radiation dosimeters. In fact, the categorization of materials into TLD vs OSLD is somewhat artificial because most materials can exhibit both TL and OSL signals. For example, Al_2O_3:C has been used as both TLD and OSLD.[22] However, in general, materials have clearly superior properties when used with either thermal or optical stimulation.

For both TLD and OSLD, different types of LDs have different properties. A partial list of the more commonly used TLD and OSLD materials and some key relative properties are presented in Table I. LiF:Ti, Mg (TLD-100) and Al_2O_3:C (nanoDot^{TM}) have characteristics that make them well suited to general dosimetry in radiotherapy environments, and specific evaluations of detector performance through this report is based on these two dosimeters. Other LDs have properties that may make them particularly well suited, or not, to specific applications. For example, TLD-100H has very high sensitivity and is well suited to low-dose applications. TLD-600 (neutron sensitive) and TLD-700 (neutron insensitive) can be coupled to measure the thermal neutron dose.[23] Thermoluminescent dosimeters based on calcium are highly sensitive for very low-dose applications in the mGy range,[24,25] but are relatively uncommon in routine medical applications because of their substantial energy dependence.

Table I lists commercial names common in North America. Different variants of these detectors are available in different regions from different manufacturers. For example, in addition to TLD-100, LiF:Mg,Ti is also produced in Europe as MTS-N with slightly different concentrations of dopants. TLD-100 and MTS-N behave equivalently for practical applications,[26] but differences do exist in terms of glow curve structures and relative trap heights.[27]

The values in Table I are only rough estimates; actual values may depend on the batch and may also depend on the form of the crystal (see Section 4 for more details). However, general characteristics, techniques for determination of correction factors, and dose formalisms established in this report should be broadly applicable to any LD materials.

The dosimetric properties of a TL/OSL detector are affected by the nature of the defects involved in the TL/OSL process and are not based solely on the host material. The density, distribution, and energy-depth of defects will directly affect characteristics such as sensitivity. This is most obviously seen when comparing TLD-100 and TLD-100H, which are both based on LiF, but because of the different dopants

TABLE I. Thermoluminescent dosimeter (TLD) and optically stimulated luminescent dosimeter (OSLD) materials available commercially along with example commercial names, density ρ, effective atomic number Z_{eff}, temperature of the main TL peak, and typical emission wavelength, sensitivity relative to LiF, beam quality dependence (k_Q; response at 30 keV vs that in cobalt), and fading. Tabulated values based on data from the literature.[2,28–31]

	Commercial names[a]	ρ (g/cm^3)	Z_{eff}[b]	Main glow peak temp[c] (°C)	Emission[d] (nm)	TL sensitivity vs. LiF	k_Q 30 keV/^{60}Co	Fading of dosimetry peak at normal temp
LiF:Mg,Ti (TL)	TLD-100	2.6	8.31	~235	~410	Referent	1.3	5% in 3–12 months
^{6}LiF:Mg,Ti (TL)	TLD-600	2.6	8.31	~235	~410	1.0	1.3	5% in 3–12 months
^{7}LiF:Mg,Ti (TL)	TLD-700	2.6	8.31	~235	~410	1.0	1.3	5% in 3–12 months
LiF:Mg,Cu,P (TL)	TLD-100H	2.5	8.31	~200	~370	30	1.25	2% in 3 months
$Li_2B_4O_7$:Mn (TL)	TLD-800	2.3	7.32	~185	~600	0.3	0.9	5–10% in 3 months
CaF_2:Dy (TL)	TLD-200	3.18	16.90	~160, 185, 245, 290	480, 575, 660, 750	30	14	25% in 4 week
CaF_2:Mn (TL)	TLD-400	3.18	16.90	~300	~495	10	14	15% in 2–4 week
$CaSO_4$:Dy (TL)	TLD-900	2.61	15.62	~220	480, 575, 660, 750	15	12	6% in 6 months
Al_2O_3:C (OSL)	nanoDot™	3.95[e]	11.28	~200	~410	N/A	3.7	4% in 3 months
BeO (OSL)	Thermalox 995	2.85	7.21	~210, 330	~335 (TL), ~390 (OSL)	N/A	0.82	5–10% in 3 months

[a]Commercial name used by Thermo Fisher Scientific, Inc. (formerly Harshaw, Inc.), Materion Ceramics, and Landauer Inc.
[b]Values from Bos.[2]
[c]These are approximate values, as the TL peak temperature varies with heating rate and may also vary considerably with impurity content and source of material.
[d]The symbol "~" indicates broad emission bands. Emission from Dy3 + in Dy-doped materials are characterized by sharp emission lines.
[e]The density of Al_2O_3 is 3.95; however, the active nanoDot crystal is powder embedded in a polyester tape and includes many air pockets.[32] The density of the active volume has been found to be in the range of 1.41–2.45 g/cm.[33,34]

and trap structures, there is a dramatic difference in sensitivity. More subtly though, because the ionization densities created by different types or energies of ionizing radiation will interact with the defects differently, the nature of the defects can also affect the energy response and linearity of the detector; TLD-100 and TLD-100H have different photon energy responses and supralinearity.[35–37] Other differences may also exist; for example, the sensitivity of TLD-100H is more influenced by the standard thermal treatments than is the sensitivity of TLD-100, thus requiring particular care.[38]

3.B. Production

LD crystals created in a distinct production run are referred to as being of the same "batch." LDs from a given batch have similar properties in terms of fading, linearity, and energy dependence. The average sensitivity from one batch to another varies substantially between production runs, potentially in excess of 20%. Further details are discussed in Section 4.

3.C. Forms

3.C.1. TLDs

Thermoluminescent dosimeters can be purchased in different forms that offer different advantages and disadvantages. The main forms are powder and solid (Fig. 4a), including rods, chips, disks, and microcubes. With powder it is possible to generate a large number of TLD with uniform characteristics. However, powder is challenging to use in terms of loading, handling, and annealing. Powder form is also sensitive to mass and powder distribution during readout. The mass of the powder is important: if the mass is too large, excessive self-attenuation of the TL occurs, which decreases the apparent sensitivity. Problems also arise for small masses. For masses <~18 mg, the signal/mass becomes dependent on the mass; therefore, only masses > 20 mg should be used. The distribution of powder on the heating pan also requires attention, as the centering and distribution of the powder can affect the signal/mass by several percent. In contrast to a powder form, solid forms can readily be annealed and reused indefinitely if appropriate procedures are followed. However, because each detector is unique, each will show variability in sensitivity that needs to be accounted for (see Section 5). Solid forms are also sensitive to being scratched or chipped, and additional care is required in their handling (see Section 8).

3.C.2. OSLDs

Optically stimulated luminescent dosimeters are commercially available only as disks or strips. For OSLDs, there is currently only one commercial material for medical applications: Al_2O_3:C. This crystal is ground into a relatively uniform powder, fixed onto a plastic tape, which is then punched into disks that are mounted into light-tight plastic cassettes [Fig. 4(b)]. Originally this was distributed as the microdot™, and the current product is the smaller nanoDot™. The readable area of the nanoDot™ is a disk 4 mm in diameter and 0.2-mm thick.

4. FACTORS RELEVANT FOR DOSE CALCULATION

Dose will most often be calculated for LDs in a manner that parallels TG-51.[40] That is:

$$D_w = M_{corr} \cdot N_{D,w} \cdot k_F \cdot k_L \cdot k_Q \cdot k_\theta \quad (1)$$

where M_{corr} is the corrected reading from the dosimeter, $N_{D,w}$ is the calibration coefficient, and each k represents a correction factor that may be necessary to relate the irradiation conditions of the high-precision calibration dosimeters (i.e., the *standards* used to define $N_{D,w}$) and the irradiation conditions of the *experimental* dosimeter. Details on each of these values are presented in the rest of Section 4.

4.A. Reading (M_{corr})

M_{raw} is the number of counts or charge per unit mass collected during a readout process. This signal is converted to the corrected reading (M_{corr}) by considering, if necessary, background signal (M_{bkg}), depletion (k_d), and individual sensitivity correction factors, $k_{s,i}$ if batch calibration is employed (see Section 5).

The background signal can be subtracted from the measured signal by reading an unirradiated LD if common background signal is expected between the background and *experimental* dosimeters. Alternately, for OSLD, the background can be assessed directly on the *experimental* dosimeter by reading the signal of the detector immediately before irradiation. For most applications, particularly in a therapy environment, background signal does not need to be determined, as it is much smaller than therapeutic doses. If very low doses are being monitored, testing for measurable background signal could be of potential value. Even in such cases though, corrections to the background signal for fading or even element sensitivity are almost certain to be unnecessary, being relatively small corrections to an already small background correction. If nanoDot™ OSLDs are reused to high doses, beyond 25 Gy, the background signal increases with time[1] and should be monitored, although specific details of such applications are beyond the scope of this report.

For TLDs, the reading process removes most of the signal, so only a single reading can be taken. For OSLDs, the reading process typically removes only a small fraction of the signal stored in the dosimeter when using readers such as the microSTAR® reader (Landauer Inc., Glenwood Il). Therefore, multiple readings can and should be made. The standard deviation of the multiple readings should be small; <1% is common,[39] even for low imaging doses.[41] Of note, both within the TG membership and as reported by the manufacturer, some users have found that if multiple readings are made successively, the first reading will be several percent higher than subsequent readings (for a 1-s read and after correcting for depletion). Because this finding is not consistent across users, the phenomenon should be investigated using multiple detectors and characterized for the specific reader, the specific holder of the OSLD disk in the reader (if applicable), and batch of OSLDs during commissioning. If a sizeable discrepancy is observed between the first reading and subsequent readings, it is most reasonable to discard the first reading — such a rejection policy must be consistently applied to all OSLD readings, including readings of *standards*.

The signal lost by each successive reading of an OSLD is accounted for with the depletion correction (k_d). Reading a nanoDot™ with a microSTAR® reader typically depletes 0.03–0.07% (k_d = 1.0003 to 1.0007) of the stored signal per 1-s reading on the high-dose scale (doses above ~ 20 cGy).[13,20,39,42,43] On the low-dose scale, for doses below ~ 20 cGy, the reader switches to a higher light intensity and each reading depletes ~ 0.25% (k_d = 1.0025) per 1-s reading.[13,43,44] Typically depletion is negligible. However, for cases such as a constancy dosimeter (see Sections 4.B and 7), numerous readings are taken so depletion is not negligible. For such a case, it must be noted that the depletion can vary substantially between the readers (Fig. 5).

The corrected signal from J total readings of an OSLD is therefore given as a function of each individual reading j as:

$$M_{corr} = \frac{\sum_j \left(M_{raw,j} \cdot k_d^{j-1}\right)}{J} - M_{bkg} \quad (2)$$

and for TLD is given as:

$$M_{corr} = \left(M_{raw} - M_{bkg}\right) \quad (3)$$

Equations (2) and (3) are the full solutions. In the common case where background signal and depletion can be neglected ($M_{bkg} \approx 0$, $k_d \approx 1$), both Eqs. (2) and (3) reduce simply to

$$M_{corr} = \overline{M_{raw}} \quad (4)$$

4.B. System calibration coefficient (N)

The system calibration coefficient (N) relates signal from the detector to the dosimetric property of interest: usually dose to water ($N_{D,w}$). This coefficient largely parallels the

FIG. 4. (a) Thermoluminescent dosimeter forms, including disks, rods, chips (top row), microcubes, disks, and powder (bottom row). (b) Optically stimulated luminescent dosimeter (OSLD) form as a nanoDot™ disk. Active volume visible as white disk in open form on the right, and OSLD enclosed in light-tight case on left.

calibration coefficient ($N_{D,w}$) for an ion chamber. However, while the calibration coefficient for an ion chamber is traceable to a primary laboratory such as NIST and is defined for very specific conditions (full ion recombination, standard temperature and pressure, etc.), the calibration coefficient for an LD is defined by the user and for the user's specific conditions, geometry, dose level, etc. The calibration coefficient for the LD should be based on a cross calibration with a calibrated ion chamber, ideally under reference conditions, to provide traceability. Similar options have been developed to provide traceability for other modalities such as brachytherapy.[45] Even so, the coefficient is not transferrable between LD readers, as different readers' sensitivities can vary by a factor of more than 2, or between different types or batches of LD, as the sensitivities of these can be substantially different as well. The reader sensitivity also changes slightly from day to day, so while it is possible to transfer this coefficient between reading sessions, this is at the cost of introducing uncertainty to the dose. This added uncertainty is approximately a few percent for typical OSLD readers but can exceed 10% for TLD readers.

The calibration coefficients for identical irradiation conditions by the Imaging and Radiation Oncology Core (IROC) in Houston are shown for a TLD reader (Harshaw model 3500) in Fig. 6(a) and for an OSLD reader (microSTAR®; Landauer) in Fig. 6(b). The data in these figures are corrected for the variability in sensitivity of each dosimeter, and show the variability in the calibration coefficient introduced by the reader itself. The calibration coefficient of the TLD reader showed variability by ±12% (coefficient of variation) over several years of readings. While some of the large changes in sensitivity were due to cleaning of the planchette, there is clearly substantial variation between days. Such variation must be accounted for to achieve reasonable accuracy in dose readings, meaning that $N_{D,w}$ must be determined for every reading session by irradiating and reading *standards* for that session. The specific OSLD reader showed much less variation: ±1.2% (coefficient of variation) but a 15% drift over 2 years [Fig. 6(b)]. There are three options to determine and maintain the calibration coefficient for an OSLD system. First, as with TLD, session-specific *standards* can be irradiated and used to determine the session-specific calibration coefficient, eliminating day to day fluctuations, and long term drift, in the OSLD reader.[42] The irradiation conditions of these *standards* can closely match experimental conditions, minimizing uncertainty. Second, by using a constancy dosimeter — a generic *standard* that is maintained over an extended period of time (and corrected for fading and depletion) to define N at the time of the session and thereby account for day to day fluctuations and long term drift of the reader. Use of a constancy dosimeter avoids additional irradiations compared to irradiating session-specific standards, but the conditions will likely less closely match specific experimental conditions and will therefore have larger correction factors and uncertainty. As a third option, because the day-to-day variability is relatively small, instead of determining a session-specific N it may be acceptable to use a single original calibration curve and accept the additional 1.2% uncertainty from day-to-day variations. Even for such an approach, a constancy dosimeter should nevertheless be maintained and used as a quality assurance (QA) check of the system to monitor for larger, long-term drifts.

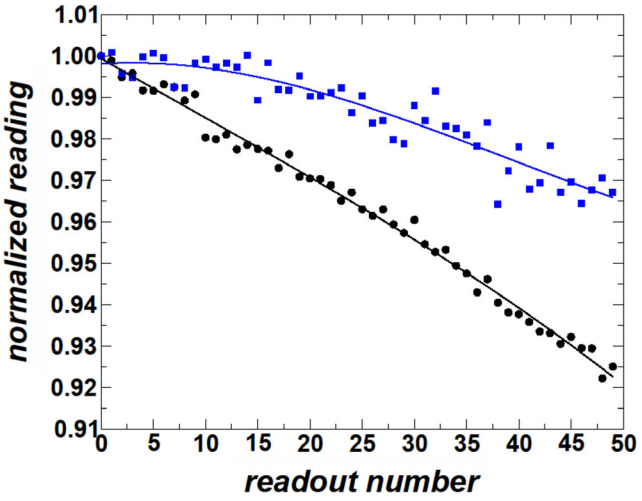

FIG. 5. Signal depletion (7 s read times, high dose scale) for a nanoDot™ optically stimulated luminescent dosimeter read on two different readers (square and circle data series), highlighting the variability between readers.

$N_{D,w}$ can be calculated as follows by irradiating *standards* to a known dose:

$$N_{D,w} = \frac{D_0}{(M_{0,corr}) \cdot k_F \cdot k_L \cdot k_Q \cdot k_\theta}, \quad (5)$$

where $M_{0,corr}$ is the corrected signal from the *standards*, and D_0 is the known dose to the *standards*. Correction factors (k), as described in the subsequent sections, are applied to this process when the irradiation conditions do not match the desired reference conditions. However, most often, the calibration conditions will define the reference conditions, and the correction factors in Eq. (5) will be unity by definition.

As implied by Eq. (5), the system calibration coefficient is defined for a specific set of irradiation and readout conditions. That is, $N_{D,w}$ is a function of parameters that affect the response of the detector. This includes energy of the beam, the time between irradiation and readout, dose, and angle of irradiation. The system calibration coefficient relates signal to dose only under these specific irradiation conditions used during calibration. For an arbitrary measurement, correction factors are required to relate the measurement conditions back to these calibration conditions where the system calibration coefficient is defined. It is also critical to note that the calibration coefficient is also defined for the specific read-out process, including the specific reader used, reader mode, heating cycle for TLD, annealing history, batch, and type of LD. For example, changing the maximum heating temperature can notably and in a nonsystematic manner affect the response of TLD, meaning that the calibration coefficient would also change.[46]

This important aspect of the calibration coefficient can be understood through a comparison to TG-51 ion chamber calibration. For the ion chamber, $N_{D,w}$ is defined on the basis of standard temperature and pressure and with zero recombination because these conditions are logical reference conditions. When the ion chamber is used in an arbitrary setting, the raw reading must be corrected back to the calibration conditions through the use of P_{TP} and P_{ion} in order to correctly apply $N_{D,w}$. For LDs, $N_{D,w}$ is also defined for a reference condition. However, there is no default reference condition, for example, no default dose level or default time between irradiation and readout. Therefore, the calibration conditions are arbitrary and will typically vary from user to user and between applications. In short, the system calibration coefficient must be understood to relate specifically to the calibration conditions used, and the measured signal under arbitrary conditions must be corrected back to those calibration conditions for $N_{D,w}$ to accurately apply.

4.C. Correction factors

Because the calibration condition and the experimental condition are rarely identical, corrections are typically necessary. The correction factors depend strongly on the type of LD (TLD vs OSLD) and on the type of TLD or OSLD. Some clinical parameters that are relevant for other detectors are not relevant for LDs, and no corrections are warranted. For example, LDs are dose rate independent within 2% up to dose rates of 4×10^9 Gy/s.[47]

Because of their abundant use in clinical practice, the values presented in this section are for TLD-100 (LiF:Mg,Ti) and nanoDots™ (Al_2O_3:C). However, the specific values shown reflect specific dosimeters and specific calibration conditions (e.g., ^{60}Co beam, readout 24 h after irradiation, etc.), which defines the normalization point for these correction factors. These factors should not be used as a replacement for commissioning of an LD system by an institution because the specific values may depend on the batch and/or reader (Table II). The values presented in this report will generally be approximately consistent and can serve as a sanity check as well as a general guide of what they are, how big they are, and how they change.

TABLE II. Dependence of the dosimetric properties of LDs on the dosimeter and reading system. An "X" in the table indicates that the property of the dosimeter is expected to change with: dosimeter type [i.e., a different type of dosimeter is used: TLD-100H vs TLD-100], specific batch of dosimeter produced, or the specific reading unit or technique used (i.e., reading system) to determine the signal.

Property	Dosimeter type	Batch	Reading system
$N_{D,w}$	X	X	X
k_d	X		X
k_L	X	X	X
k_F	X		
k_Q	X		
k_θ	X[a]		
$k_{s,i}$	X	X	X

[a]Depending on the form of the detector.

It is commonly assumed that each of the correction factors described is independent of the others. This is not strictly true for all variables; nonlinearity, for example, does vary to some degree with beam energy.[36] However, most corrections are relatively small; therefore, any cross-correlation between the correction factors is typically neglected.

It should also be noted that the correction factors can be a function of the read-out procedure; energy dependence of TLD, for example, has been found to vary with maximum read-out temperature.[46] For reasons such as this, consistent procedures should be implemented to ensure consistent results. Additionally, clear reporting of parameters is necessary in publications to allow for intercomparisons between research groups (see Section 12).

This report only presents correction factors inherent to the dosimeter. Oblique irradiation results in an elevated dose at the surface, which will be detected by a dosimeter, but this is not angular dependence of the dosimeter and is not considered as such in this report. Similarly, changes in response of the detector because of the presence of wedges, extended SSD, or field size are actually examples of the energy response of the dosimeter and are discussed in that section. In addition, it is possible for the reader itself to have nonlinearities in response as a function of signal in addition to those

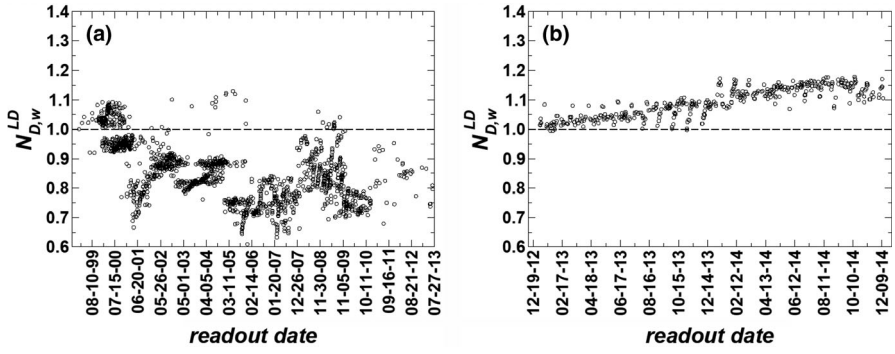

FIG. 6. Variation in system calibration coefficient ($N_{D,w}$ relative to $N_{D,w}$ determined on the first day) as a function of day for a Harshaw model 3500 reader (a) and a Landauer microSTAR® reader (b).

of the detector. In one Harshaw reader, nonlinearity approached 5%[48]; such an effect should ideally be directly corrected for, or if a consistent dosimeter and reading process is applied, could be encompassed into the nonlinearity response of the dosimeter.

4.C.1. Linearity correction (k_L)

The signal/dose of LDs depends slightly on dose. Of note, this section describes the response to dose from individual irradiations — accumulated dose following cycles of reuse of the detector (i.e., cycles of annealing/bleaching to "zero" the signal of the detector) is discussed in Section 10.

At low doses, LDs show a linear response with dose; as the dose increases the response becomes supralinear; and finally, at very high doses, the response becomes flat (as all of the traps are filled). The linearity correction accounts for the change in sensitivity of the LD with delivered dose. It is defined as equal to 1 at a user defined reference dose (D_{ref}) and is then described by Eq. (6) for the dose and signal associated with an experimental dose (D_{exp}).

$$k_L(D) = \frac{D_{\exp}}{M(D)_{\exp}} \Big/ \frac{D_{ref}}{M(D)_{ref}} \tag{6}$$

Linearity is characterized by irradiating *standards* over a range of doses and assessing the response per unit dose. The range of doses should cover the reference dose in Eq. (6) so that this normalization point is well sampled. Other corrections, such as fading and energy, should be controlled during this characterization by ensuring all irradiations and readouts are done on the same time cycle and at the same beam energy.

For TLD-100, nonlinearities are small over the dose range up to 2 Gy, being linear within an uncertainty of ±2.5% (1-sigma).[49,50] For the nanoDot™, nonlinearities are presented in Fig. 7 and are clear by 2 Gy, increasing to ~15% by 10 Gy.[43] Care is required for this correction factor. Nonlinearity effects are substantial enough that the variations in linearity may be seen between batches and could vary with reader (Table II). To maximize precision, this effect should be characterized or verified for new batches (see Section 7). Different reading systems will not generally impact the nonlinearity.

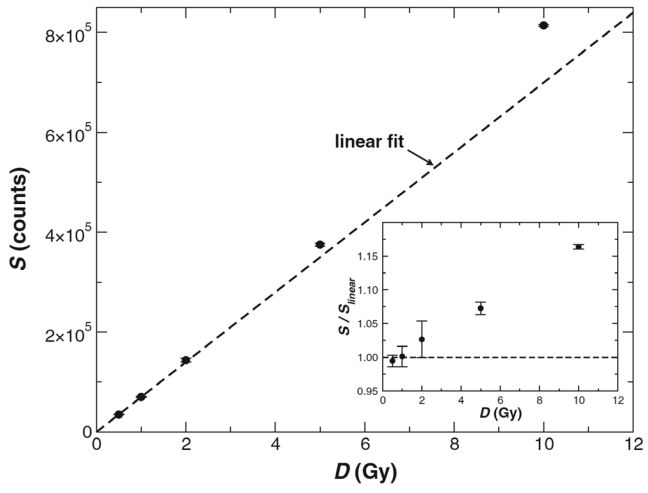

FIG. 7. Supralinearity response of optically stimulated luminescent dosimeters [signal (S), corresponding to M in this report, vs given dose (D)]; the increased response relative to linearity is seen in the residual plot (insert). Reproduced with permission from Omotayo et al.[43]. Similar behavior is seen with thermoluminescent dosimeters.

k_L can be minimized by using low doses, by annealing/bleaching the detectors if they are being reused to remove existing signal, and/or by irradiating *standards* to the same dose as *experimentals* (such that $k_L = 1$ by definition). Otherwise, or to improve accuracy, a correction factor can be determined and applied (as, for example, the inverse of the data shown in Fig. 7). The relationship between signal/dose and dose (i.e., linearity) is also captured when a calibration curve is generated — that is, determining detector response over a range of doses.

For nanoDot™ OSLD, it has been suggested that k_L can vary not just with dose, but also individually between dosimeters (even within a single batch of nanodots™).[1] However, the preponderance of the published literature[21,42,43]) has found no indication of this effect and suggests that all dosimeters of a single batch can reasonably be assumed to have the same nonlinearity characteristics, at least up to 10 Gy. At doses beyond 10 Gy, k_L can change substantially depending on the dosimeter's dose history [1], that is, whether or not the dosimeter has been previously bleached. The complications of this situation, together with the changes in sensitivity, are a major obstacle in using this dosimeter beyond 10 Gy.

4.C.2. Fading correction (k_F)

Signal is lost by LDs as a function of time because of the spontaneous (thermally stimulated) escape of trapped electrons at room temperature. The fading correction compensates for the decrease in signal that occurs between irradiation and reading. Fading occurs logarithmically, and so is most pronounced immediately after irradiation and becomes less pronounced with time. It is described with Eq. (7) for the time between irradiation and readout for the experimental condition ($M(t)_{exp}$) vs the reference condition ($M(t)_{ref}$).

$$k_F(t) = \frac{D_{\exp}}{M(t)_{\exp}} \Big/ \frac{D_{ref}}{M(t)_{ref}} \tag{7}$$

In defining k_F, all variables other than time between irradiation and readout should be kept as close to constant as possible between the experimental and reference conditions. It is very likely, therefore, that D_{exp} and D_{ref} are equal.

TLDs are read after a preread heating phase, during which the shallowest and highly unstable traps are emptied. Consequently, fading for TLDs describes the loss of signal from deeper, more stable, dosimetric traps. For TLD-100, fading is on the order of a few percent over the first few days, and then approximately one percent per month.

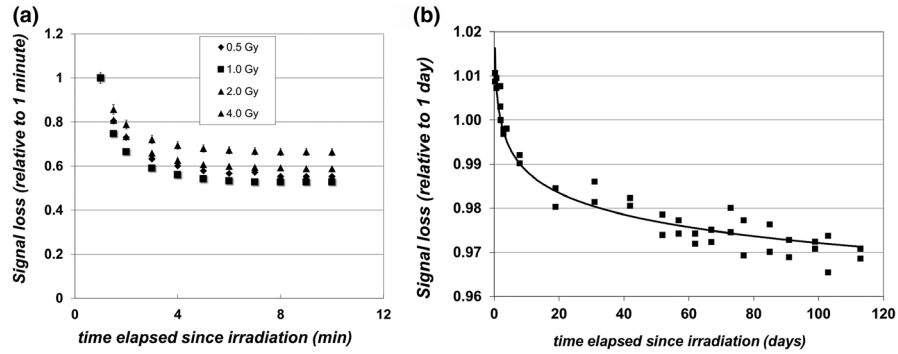

FIG. 8. Signal loss vs time ($1/k_f$) on two time scales. a) Pronounced fading of the nanoDot™ OSLD signal during the first 10 minutes postirradiation (based on data in ref [51]. b) Long-term signal loss for the nanoDot™ OSLD over several months (relative to 1 day). LiF thermoluminescent shows a similar long-term signal loss as in panel (b).

OSLDs, in contrast, do not have their unstable shallow traps emptied before reading. Consequently, their fading includes this loss of signal; nanoDot™ OSLDs show 30-40% signal fade during the first ~8 min postirradiation as the shallow traps spontaneously empty[20,51] (Fig. 8). After these first 8 min of substantial instability, only dosimetric traps remain filled and the signal is much more stable so that fading is on the order of a percent per month. nanoDots™ should not be read within 10 min of irradiation.

Because of the logarithmic nature of fading, the signal is more stable after more time has passed postirradiation. Therefore, normalizing the signal to a short time postirradiation is less precise. However, these longer times rarely meet clinical needs. Reasonable minimum wait times are 12 h for TLD-100 and 10 min for nanoDot™ OSLD LDs.

If irradiation and readout times can be reasonably controlled, k_F can be minimized by ensuring the time between irradiation and readout is the same for both the *standards* and *experimental* LDs. In such a case, the same signal is lost from both the *experimentals* and the *standards*, and k_F is unity. Otherwise, fading can be corrected for by characterizing the fading over the time period of interest (such as Fig. 8), where k_f is the inverse of the data.

While fading varies with dosimeter type (Table I), the experience of the task group members is that it does not meaningfully change between batches of the same dosimeter, and it is not a function of the reading system used (Table II).

4.C.3. Beam quality correction (k_Q)

As beam quality changes, the detector response changes as well. The correction to this change in response is described by k_Q. LDs actually show two types of energy dependence:

First is intrinsic energy dependence ($k_{Q,int}$). This is a property of the LD itself, and is the change in the relationship between the dose to the detector and the signal from the detector as beam quality changes. For TLD-100, this component of the energy dependence can contribute up to 1/2 of observed energy dependence down to energies as low as 200 keV.[52] Of note, this mechanism relates to how the microscopic dose distribution created by particles of different energies influence the trapping and recombination mechanisms. As such, this component of the energy dependence cannot be captured by Monte Carlo or cavity theory considerations but must instead be determined empirically. There is no current indication that Al_2O_3:C OSLDs show an intrinsic energy dependence in excess of 1–2%, even down to a few hundred keV.[53,54]

Second is medium-dependent energy dependence ($k_{Q,m}$). This is the change in the relationship between the dose to the detector's material and the dose to surrounding medium (usually tissue) as the beam quality changes. This is relevant because LDs are used as cavities in a different medium (usually tissue) to determine the dose to that medium. The energy dependence arises because of differences in the mass attenuation coefficients and stopping power ratios between tissue and the detector materials. This is the dominant component of the energy dependence of LDs and appears to be the only component for Al_2O_3:C, except for very low-energy photons (<100 keV).

Practically, these two energy-dependent factors are rarely separated, and only a single energy-dependent factor (the product of $k_{Q,int}$ and $k_{Q,m}$) is reported: k_Q. This factor is defined as the ratio in the reading of the LD (per unit dose) to irradiation at a given energy from its response to irradiation at a reference energy (the calibration beam energy):

$$k_Q = \frac{D_{\exp}}{M(Q)_{\exp}} \Big/ \frac{D_{ref}}{M(Q)_{ref}} \tag{8}$$

In defining k_Q, all variables other than beam quality should be kept as close to constant as possible. For example, D_{exp} and D_{ref} should be very similar so nonlinearity effects are not introduced into the definition of k_Q.

There is little variation in beam quality dependence for TLD-100 or nanoDots™ across megavoltage photons (^{60}Co–18 MV) and electrons (5–22 MeV). Both of these dosimeters have nearly identical relationships: compared to the response at 6 MV, the LD's response in cobalt is around 2% higher and typically <1% difference in response is seen across different high-energy photon beams. The response in electron beams is around 2% lower for all energies compared to a

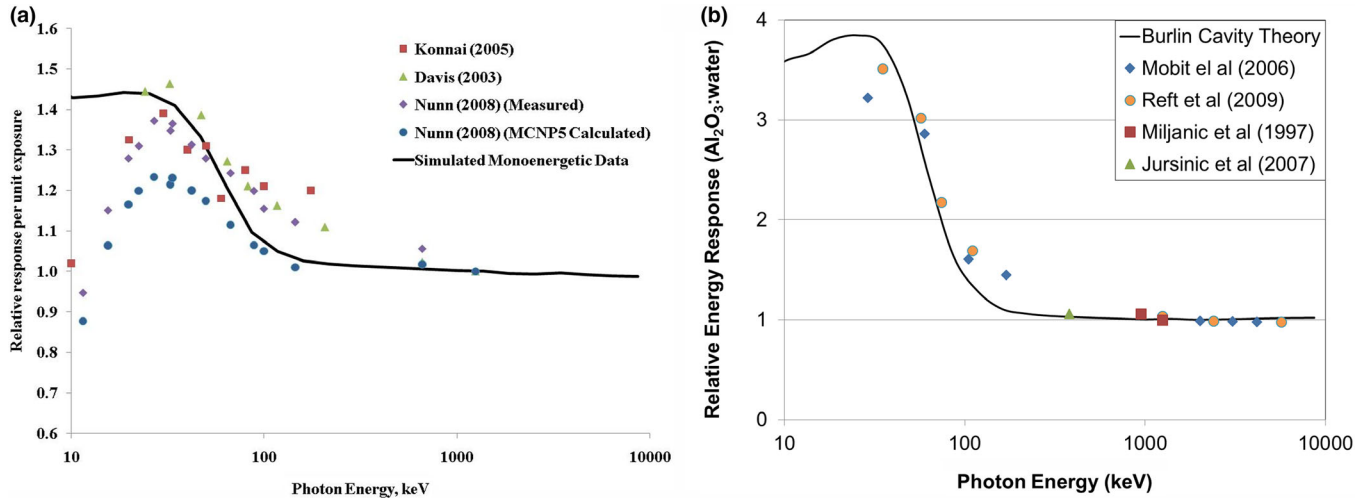

FIG. 9. Relative response ($1/k_Q$) vs beam quality for (a) TLD-100 (reproduced with permission from Scarboro et al[52] and (b) nanoDots™ (based on reference.[59] Note the substantially different y-axis scales.

6 MV beam.[12,20,51,55–57] However, at lower energies, the response of LDs can be drastically different from that at MV levels: the over-response can exceed 40% for TLD-100 and exceed a factor of 3.5 for Al_2O_3:C (Fig. 9) in low-energy photon beams. Simultaneously, with very low-energy photons, self-absorption by the LD crystal also becomes an issue, and the relative response of LDs actually decreases at very low energies because of this [Fig. 9(a)]. The complex response at low energies may be very relevant for clinical applications including brachytherapy (see Section 11.D).

While LDs have an increased response to low-energy photon beams because their mass energy absorption coefficients increase relative to water, this is not mirrored with low-energy electrons. The relative mass stopping power between water and LiF or Al_2O_3 changes minimally with energy, actually decreasing at lower energies,[58] so LDs may under-respond to low-energy electrons.

Beam quality correction factors in the clinic are minimized if *standards* and *experimentals* are irradiated at the same nominal energy. Otherwise, the relative response of the detector between different energies can be determined during commissioning and corrected on a case by case basis. Of note, the nominal energy does not specify the radiation quality at all points inside or outside of that radiation field. Irradiations with a 6-MV beam under noncalibration conditions (e.g., modulated fields, presence of wedges, large fields, etc) can affect the spectrum[52,53,60,61] and therefore the response of the dosimeter. Within the treatment field, this impact is <1% for TLD-100 and <3% for nanoDot™ LDs; however, outside the treatment field, this effect can exceed 10% (TLD) or 30% (OSLD).[52,53] This issue is particularly pronounced for some kV sources, such as ^{192}Ir, where the photon spectrum changes dramatically as the beam penetrates material.

Beam quality dependence varies with dosimeter type (Table I). However, the experience of the task group members is that it does not meaningfully change between batches of the same dosimeter, and it is not a function of the reading system used (Table II).

4.C.4. Angular correction (k_Θ)

The angular correction takes into account any difference in signal because of the angle of incidence of the experimental beam on the detector compared with the angle of incidence of the calibration beam. Angular dependence refers strictly to the inherent response of the dosimeter. If the detector is placed on a patient surface, for example, an oblique beam will deliver more dose to the surface (and therefore to the detector) than a normally incident beam. This is not angular dependence of the dosimeter, although it is an effect that may require consideration.

At therapeutic energies, there is no evidence of angular dependence for TLD for common forms such as chips or rods. Angular dependence is a potential issue for low-energy photons (e.g., below 30 keV) where self-attenuation of the TLD becomes an issue and asymmetry in the shape of the dosimeter can therefore affect the response. At diagnostic energies, Struelens et al.[62] reported a 2% decrease in the response of a TLD chip oriented at 60° from the vertical, increasing to a 10% decrease at 90°. For ^{125}I radioactive seeds, Mobit and Badragan reported a 3% change in the response of LiF microrods over a change of 90°.[63]

Current commercial OSLDs are in a disk-type form, which can introduce angular dependence for geometrical reasons when comparing an edge-on irradiation to an en-face irradiation, as electrons may preferentially scatter out of the thin but relatively high-density disk with an edge-on irradiation. At megavoltage energies, mixed results have been found between edge-on and en-face signal per dose, ranging from 0% to 1%,[20] 2% [33], and 4%[64,65]). Detailed Monte Carlo simulations supported that there is a 2% effect at 6 MV.[33] At lower energies, angular dependence has been found to increase for the nanoDot™, although the results in the literature are not always consistent. A 4% angular dependence effect was observed for Ir-192,[66] and a 3%–16% effect in diagnostic CT beams (80–140 kV).[41] Angular variation of 40% at 80 kVp and of 70% in a mammography beam[44] have

also been reported. More study on angular dependence at low energies is warranted.

Angular dependence can vary with dosimeter form (Table I). As it is a physical property of the detector, it does not meaningfully change between batches of the same dosimeter and is independent of the reading system used (Table II). Because it is a physical geometry effect, the angular effects need not be characterized for individual LD programs when the same shape of detector has already been evaluated.

5. BATCH CALIBRATION

The term "batch" can refer to two different groupings in LD applications. A batch of TL/OSL crystal refers to a single production run of crystal (as with other detectors such as film). However, it can also be used to describe a group of detectors that have been commissioned together to form a batch. A group of detectors that have been commissioned together to be a practical batch of detectors should all come from the same production run of crystal.

In a batch calibration approach, all of the dosimeters in the batch are assumed to have uniform characteristics except individual element sensitivity: $k_{s,i}$. Fading, energy response, linearity, angular dependence, etc., are applied uniformly to all elements in the batch, and $N_{D,w}$ is the average system calibration coefficient of the batch (at least for that given reading session). This assumption of uniform dosimeter characteristics requires that the detectors commissioned as a batch all come from the same detector production run, otherwise the assumption will be inaccurate as described in Table II.

When the detectors have been commissioned as a batch, it is still generally necessary to consider and manage the variability in the sensitivity of the different elements of the batch compared to the average. This is described with the element sensitivity correction factor: the ratio between the mean response of the batch ($\overline{M}$) and the individual dosimeter response (M_i), and can be determined by exposing all dosimeters to a uniform dose and comparing individual signals to the mean signal.

$$k_{s,i} = \frac{\overline{M}}{M_i} \tag{9}$$

If TLD powder is used (provided the powder is uniformly mixed), all TLDs are identical (per unit mass) and $k_{s,i}$ is unity (per unit mass of powder).

For solid forms of LDs, each dosimeter will have a unique sensitivity because of variations in concentrations and in distributions of impurities and traps, and for nanoDot™ OSLD the different masses of crystal cannot be accounted for by weighing the sensitive volume because it is inaccessible. In this case, the element sensitivity can be managed in one of two ways. First is to determine and apply $k_{s,i}$ for each dosimeter. This can be logistically challenging but provides maximum precision and is facilitated with nanoDot™ OSLD, which have a unique bar code attached to the detector. The second option is to define a $k_{s,i}$-window (e.g., within ±3% of the mean sensitivity), and when the batch of LDs are commissioned, only those whose sensitivity is within that window are accepted as part of the batch. In this case, no individual $k_{s,i}$ correction is identified or applied, and dose measurements correspondingly have an additional uncertainty that is approximately the size of the window. Determining which detectors fall within the $k_{s,i}$ window is often performed by the user but can also be conducted by the manufacturer as in the case of "screened" nanoDots™. If detectors such as these are purchased to be within a certain window, the agreement of detectors with that window should be spot-checked to verify (for ≥ 5% of the sample). Using a $k_{s,i}$-window decreases the precision of the dosimeters (and rejects dosimeters outside the window) but makes workflow simpler as there is no correction to track or apply.

In general, there can be substantial variation between elements. Unscreened nanoDot™ OSLDs show a coefficient of variation of around 2.2% in their sensitivities (Fig. 10).[39,42] As $k_{s,i}$ can exceed 10% for individual elements, it is important that this factor be accounted for.

Physical damage to a TLD or OSLD, such as chipping or scratching, can substantially affect its $k_{s,i}$. The element sensitivity correction should be re-evaluated if such damage occurs.

If $k_{s,i}$ is individually tracked for the dosimeters, this is incorporated into M_{corr} as follows for the *ith* OSLD read J times:

$$M_{corr} = k_{s,i} \cdot \left[\frac{\sum_j \left(M_{raw,j,i} \cdot k_d^{j-1} \right)}{J} - M_{bkg} \right] \tag{10}$$

and for the *ith* TLD:

$$M_{corr,i} = k_{s,i} \cdot \left(M_{raw,i} - M_{bkg} \right) \tag{11}$$

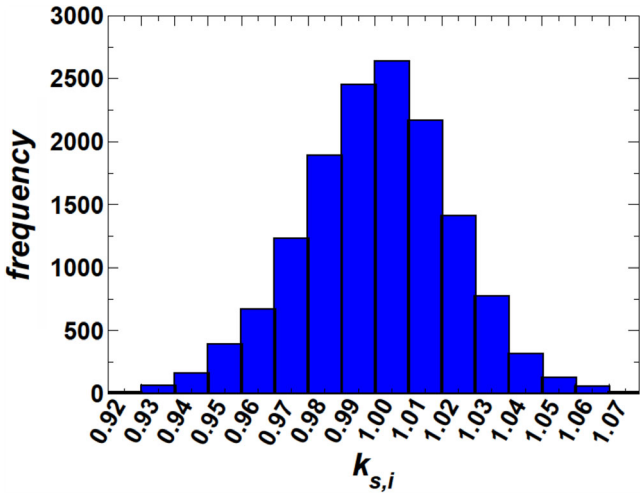

FIG. 10. Distribution of $k_{s,i}$ values for unscreened nanoDot™ OSLD, highlighting that this correction factor can be substantial.

Both Eqs. (10) and (11), paralleling the reduction to Eq. (2), most often reduce to:

$$M_{corr,i} = k_{s,i} \cdot \overline{M_{raw,i}} \quad (12)$$

As highlighted in Table II, the element sensitivity factor can vary based on the type of reader used, and should be recharacterized if the reading system is changed.

6. DOSE CALCULATION FORMALISMS

The calculation of dose for the LD system is based on Eq. (1). However, when establishing an LD program, different options are available in terms of selection of which correction factors to consider and the methods to determine the correction factors. Multiple reasonable options exist depending on the level of desired accuracy. Here we describe two methods: first, a high-accuracy approach that maximizes precision and accuracy but requires additional time in commissioning and for use, and second, a high-efficiency approach that provides lower precision and accuracy but offers a time and effort advantage. Choice of which formalism to implement depends on the clinical workflow and desired accuracy. However, when setting up a program, these two formalisms also require different commissioning procedures, which can make it very challenging to move between them if one suddenly wants more or less accuracy. Appropriate quality assurance as described in Section 7 is also necessary for either formalism to ensure the reading process is accurate.

As these dosimeters have been most often used in megavoltage therapy applications, the protocols and uncertainties are based specifically on these applications. Other applications, such as brachytherapy or imaging applications, will largely follow these calibration processes, but additional considerations and larger uncertainties are generally warranted, as discussed in Section 11.

6.A. High accuracy

In a high-accuracy approach, both commissioning and measurements are designed to minimize uncertainty. This approach is widely used by groups such as IROC Houston, the International Atomic Energy Agency (IAEA), and the Australian Calibration Dosimetry Services (ACDS), as described in associated publications,[42,67–69] and is very similar between both TLD and OSLD.

6.A.1. Commissioning

Characteristics of the dosimeters (linearity, fading, beam quality, and depletion for OSLD) are quantified over the range of values that will be encountered during measurements. Correction factors/functions (such as shown in Figs. 7 and 8) are established to relate the signal under different irradiation and readout conditions. Angular effects can be reasonably estimated from Section 4.C.4. The difference in individual dosimeter sensitivity must be carefully managed: for TLD, a very tight k_{si}-window is applied to ensure uniformity. For OSLD, each detector response is individually tracked, usually by applying a batch calibration, using the average $N_{D,w}$ for the batch, and determining $k_{s,i}$ for each detector. Alternatively, high-precision measurements can be achieved without using a batch approach by using an individual calibration coefficient for each detector. However, the latter approach may be not practical for high-volume programs.

6.A.2. Measurement, general

For OSLD, each detector is read multiple times and corrected for depletion. For TLD, each detector is read a single time because the reading is destructive.

6.A.3. Measurement, calibration

The calibration coefficient ($N_{D,w}$) is determined uniquely for each reading session. It is determined by carefully irradiating and reading at least two *standards* for the session. These *standards* are irradiated to minimize the difference between the calibration condition and the experimental condition (i.e., to the degree reasonable, the *standards* and the *experimentals* should be irradiated to the same dose, at the same time, with the same beam quality, and with the same detector orientation to minimize the correction factors and therefore the uncertainty in the correction factors needed for the experimental detectors).

6.A.4. Measurement, experimental

The experimental dose is measured with multiple detectors (at the same time). Each correction factor (k_F, k_L, k_Q, k_θ) is applied as appropriate (although the values should be close to unity by design) to correct any differences between the calibration condition and the experimental condition (e.g., if the *standards* were irradiated 3 days before readout while the *experimentals* were irradiated 2 days before readout, a k_F correction should be applied to correct for signal loss between day 2 and 3).

6.B. High efficiency

A high-efficiency approach is commonly employed in clinical practice,[70] and is recommended by some OSLD manufacturers (Landauer). Naturally, the trade-off is larger uncertainty than that achievable with the high-accuracy approach. To improve efficiency, different methods are employed for TLD vs OSLD, and correspondingly the high-efficiency approach is different in some aspects between the two detectors as described below.

6.B.1. Commissioning

A calibration curve is established by irradiating the *standards* over a range of doses using the most common beam

energy. This establishes $N_{D,w}$ and k_L together. Additional LDs are exposed to known doses from other beam energy/modalities to check that the magnitude of k_Q is within acceptable limits (i.e., no correction is warranted). A standard irradiation-to-readout time window is also established, and tested via exposing/reading additional LDs throughout that time window to check that the magnitude of k_F is within acceptable limits (i.e., no correction is warranted). Acceptable limits on k_Q and k_F are defined by the end user, who will use them when estimating the uncertainty in his/her particular setup. Angular effects are generally ignored, but can be reasonably estimated from Section 4.C.4. For TLD, the variability in individual dosimeter sensitivity is most often managed by exposing all detectors to a known dose then selecting for clinical use only those detectors within a $k_{s,i}$-window (responses within, for example, ±5% of each other). The individual sensitivity of each TLD is not tracked, rather a single calibration coefficient is used for all detectors and $k_{s,i}$ is assumed to be unity. For OSLD, the variability in individual dosimeter sensitivity can be managed following a similar approach to TLD and establishing a $k_{s,i}$-window, but it is more often managed by using "prescreened" OSLDs. Each prescreened nanoDot™ is provided by the manufacturer with a unique $k_{s,i}$, and an associated uncertainty. A Constancy Dosimeter (*standard*) is also established for OSLD to verify the stable functioning of the dosimetry system postcommissioning. Depletion (k_d) is characterized for the Constancy Dosimeter by repeatedly reading it. Depletion is typically ignored for routine clinical measurements, the uncertainty introduced by this can be easily estimated from the depletion study conducted for the Constancy Dosimeter.

6.B.2. Prescreened OSLD

Prescreened nanoDots™, where the sensitivity is reported by the manufacturer, are commonly used. However, because dosimetry programs using these detectors typically intend to only irradiate and read them a single time (with no bleaching), it is not possible to verify the manufacturer-supplied sensitivity. Therefore, upon receipt of detectors, their sensitivity (as reported by the manufacturer) should be verified for 5% of the received sample by measuring their response to a known dose.

6.B.3. Measurement, general

For OSLD, each detector is read multiple times, but depletion is generally ignored (except for the Constancy Dosimeter as described below). For TLD, each detector is read a single time.

6.B.4. Measurement, calibration (OSLD)

No session-specific calibration coefficient ($N_{D,w}$) is determined. Rather, the calibration curve established during commissioning is used. This curve is, however, verified for each session with the constancy dosimeter (or scaled according to the constancy dosimeter reading). This constancy OSLD is corrected for depletion and fading due to its repeated reading and long life span. The depletion correction is based on the commissioning data. Fading for this application can be taken from Fig. 8(b) as a reasonable estimate provided the time duration is not overly long. Therefore, a new constancy dosimeter should be established periodically (see Section 7) by exposing an OSLD to a known dose under highly controlled conditions.

6.B.5. Measurement, calibration (TLD)

For TLD, because of the potential variability in the reader (Fig. 6) and changes in batch sensitivity that can occur with repeated annealing, at least two *standards* should be irradiated to normalize the calibration curve (i.e., to define a session-specific $N_{D,w}$), although the precision of such a measurement may be less rigorous than in a high-accuracy setting (e.g., the *standards* could be irradiated at a markedly different time than the *experimentals*).

6.B.6. Measurement, experimental

The experimental dose is typically measured with a single detector. Fading, beam quality, and angular corrections are ignored, as long as the beam qualities and time-delays remain within the range tested and deemed acceptable during commissioning. Irradiation with beam qualities and time-delays that have not been tested will increase uncertainty and could lead to serious errors.

6.C. Associated uncertainties

The two formalisms described above have different commissioning processes and different application and management of correction factors and will therefore have different uncertainties. In addition to this, the uncertainty is also impacted by the nature of the detector's use. This use could be a very controlled setting, for example, a highly experienced operator and tightly restricted measurement conditions, such as linac output verification, where the experimental conditions very closely match the reference/calibration conditions. This use could also be a much less controlled setting, for example, a less experienced operator and more general measurement conditions, such as arbitrary treatment dose verification or delivery of a complex treatment from many angles, where the experimental conditions do not match the reference conditions as closely.

Uncertainty estimates (including Type A and Type B uncertainties) for the calibration formalisms described above, and for a range of controlled vs less controlled conditions within each formalism, are presented in Tables III and IV. Any specific dosimetry protocol implementation and/or application could have an associated uncertainty anywhere within (or even outside) this range. Importantly, these

TABLE III. Uncertainty budget (%) for OSLD nanoDots™. Four uncertainty budgets are considered based on a high-accuracy or high-efficiency calibration (as discussed in Section 6.A and 6.B) and for experimental use of the dosimeter in a "controlled" setting (restricted measurement conditions and an experienced operator) as well as a less-controlled setting (more general measurement conditions and a less experienced operator).

	OSLD			
	High accuracy		High efficiency	
Variable	Controlled	Less controlled	Controlled	Less controlled
D_0	0.6	0.6	0.9	0.9
M_0	0.8	1.6	1.4	2.0
$M_{raw} \cdot K_{s,i}$	0.8	1.6	2.8	2.9
k_L	0.3	0.6	0.3	0.6
k_F	0.1	0.2	1.0	2.0
k_Q	0.9	2.2	1.0	2.2
K_θ	0.0	1.0	0.0	1.0
Total (1-sigma)	1.6	3.4	3.5	4.9
Total (2-sigma)	3.2	6.8	7.0	9.7

TABLE IV. Uncertainty budget (%) for LiF:Ti,Mg thermoluminescent dosimeters (TLD-100). Four uncertainty budgets are considered based on a high-accuracy or high-efficiency calibration (as discussed in Section 6.A and 6.B) and for experimental use of the dosimeter in a "controlled" setting (restricted measurement conditions and an experienced operator) as well as a less-controlled setting (more general measurement conditions and a less experienced operator).

	TLD			
	High accuracy		High efficiency	
Variable	Controlled	Less controlled	Controlled	Less controlled
D_0	0.6	0.6	0.9	0.9
M_0	0.7	0.7	1.0	1.4
M_{raw}	1.7	1.7	1.7	2.0
k_L	0.1	0.2	0.1	0.2
k_F	0.7	1.4	1.0	2.0
k_Q	1.1	1.5	1.0	1.4
$K_{s,i}$	0.0	2.0	2.5	2.5
K_θ	0.0	0.0	0.0	0.0
Total (1-sigma)	2.3	2.8	3.6	4.4
Total (2-sigma)	4.7	5.7	7.2	8.7

uncertainty estimates reflect the technical uncertainty in the dosimeter. Matching measured doses with, for example, treatment planning system doses for *in vivo* dosimetry also includes uncertainty from the TPS calculation as well as inaccuracy in dosimeter placement. These additional sources of error are not included in the below tables, but can be the dominant source of uncertainty, particularly for *in vivo* dosimetry.[70] This is discussed more in the specific applications of Section 11.

6.C.1. OSLD

High accuracy: The uncertainty in the controlled use situation is taken from Alvarez[69] and includes uncertainty in the dose to the *standards* (based on ^{60}Co), uncertainty in the OSLD reading process, and the uncertainty in the underlying correction factors (assuming they are close to unity and therefore the uncertainty in their values is small). In this process, the uncertainty in $k_{s,i}$ (for batch calibration) is included in the uncertainty in M (and M_0). Normal incidence on the detector is assumed such that there is no angular dependence. The uncertainty of 1.6% reflects the uncertainty quoted by agencies such as IROC Houston and IAEA for highly controlled beam-calibration verification measurements.

The less controlled situation expands on the uncertainties in the controlled situation on the basis of an assumed 1% additional noise in the OSLD readings (M_0 and M), as can be observed with a less experienced reader. The uncertainty in the fading and linearity correction factors is doubled to account for larger correction factors necessary for a larger range of doses and timings that could be encountered. This method also assumes a 2% increase in the uncertainty in the energy correction to account for variations in beam energy as field size and other treatment parameters vary (which changes the response of the detector but cannot usually be accounted for with a correction factor).[53] The uncertainty for the less controlled scenario also assumes that the OSLD is irradiated from a variety of angles but that no angular dependence correction factor is applied. The estimated uncertainty here is consistent with that reported from clinical irradiations.[71]

High efficiency: In the controlled-use situation, it is assumed that the calibration is conducted on a linear accelerator. The uncertainty in the reading of the *standards* is increased as a single calibration curve is used rather than determining a session-specific calibration (i.e., a session-specific $N_{D,w}$) resulting in ~1.2% day-to-day variations in reader sensitivity (incorporated into M_0). The uncertainty in the fading correction is larger because of the assumption that fading is not accounted for (but this uncertainty is still minimized by controlling the time between irradiation and readout for *standards* vs *experimentals*). There is uncertainty in k_Q because a single calibration curve is used for all megavoltage energies. It is also assumed that screened nanoDot™ LDs have been used, for which the manufacturer offers a ±5.5% specification (at the 2-sigma level) on the sensitivity + readout (i.e., combined $k_{s,i}$ and M_{raw}). Normal incidence on the detector is assumed such that there is no angular dependence.

The less controlled situation expands on the uncertainties in the controlled situation on the basis of an assumed 1% noise in the OSLD readings (M_0 and M) associated with a less experienced reader. A doubling of uncertainty in the fading and linearity correction factor is assumed to account for larger correction factors associated with a larger range of doses and time periods between irradiation and readout. The uncertainty in k_Q is estimated to be 3%, assuming that a single calibration curve has been generated for, and used for, all

energies: 1% accounts for variations between nominal beam energies[42] and 2% accounts for variations in energy response as field size and other treatment parameters vary.[53] The less controlled uncertainty also assumes that the OSLD is irradiated from a variety of angles but that no angular dependence correction factor is applied.

6.C.2. TLD

High accuracy: The uncertainty in the controlled situation is taken from Kirby et al.[67] and includes uncertainty in the dose to the *standards* (based on ^{60}Co), uncertainty in the TLD reading process, and uncertainty in the underlying correction factors. The irradiation conditions are assumed to be controlled such that the correction factors are close to unity, and therefore have small uncertainties. This uncertainty also assumes that uniform TLD powder is used ($k_{s,i} = 1$ for all dosimeters). The uncertainty of 2.3% reflects the uncertainty quoted by agencies such as IROC Houston, the University of Wisconsin Medical Radiation Research Center, and the IAEA for calibration measurements. The uncertainty in the TLD dose measurements is similar to that for OSLDs, with the largest difference being that the reading precision is poorer for TLDs.

The less controlled situation assumes that a solid form of TLD is used (chip or rod). In this case, the uncertainty in M_0 and M would be unlikely to change over the value associated with an experienced powder reader, so the same uncertainties are quoted. The uncertainty in the fading and linearity correction factors is doubled to account for larger correction factors associated with a larger range of doses and timings that could be encountered. A 1% increase in the energy response is included to account for variations in energy response as field size and other treatment parameters vary,[52] which cannot generally be accounted for. As solid forms are used, the TLDs are not completely uniform but will have had their sensitivities ($k_{s,i}$) grouped together within a window, assumed to be ±2%.

Thermoluminescent dosimeters are used in many forms, and the uncertainty may vary slightly between them. Powder provides uniform crystal so there is no $k_{s,i}$ correction to apply; in contrast, with a solid form sensitivities will generally need to be grouped and therefore have uncertainty in $k_{s,i}$. On the other hand, powder is more prone to uncertainty in the readout process, leading to a larger uncertainty in M and M_0, particularly with inexperienced operators. Powder typically has uncertainties greater than 1%, while reading reproducibility has been reported to be as good as 0.3% for TLD-100 chips and about 0.6% for TLD-100 microcubes at the 1-sigma level.[72]

High Efficiency: In the controlled situation, the calibration is assumed to be conducted on a linear accelerator rather than a ^{60}Co unit, and therefore the uncertainty in D_0 is larger. A single calibration curve is used for all energies, but the reference energy is 6 MV so the overall uncertainty in k_Q is comparable. The uncertainty in the fading correction is larger than in the high-accuracy formalism because the time between irradiation and readout of the *standard* and *experimental* is more varied. It is also assumed that a $k_{s,i}$-window of ±5% (at the 2-sigma level) has been applied.

The less controlled situation expands on the uncertainties in the controlled situation on the basis of an assumed 1% noise in the TLD readings (M_0 and M) associated with a less experienced operator. A doubling of uncertainty in the fading and linearity correction factor is assumed to account for larger correction factors associated with a larger range of doses and time periods between irradiation and readout. A 1% increase in k_Q is included to account for variations in energy response as field size and other treatment parameters.[52] The same individual element sensitivity window ($k_{s,i}$) is assumed used in the less controlled situation.

7. COMMISSIONING AND QA

The recommendations below are made for a generic clinical setting, and should be adapted by individual physicists according to the needs of their particular clinics. As discussed in Section 6, users will have different levels of desired accuracy and precision. Acceptance criteria in Tables V–VIII are based on the analysis of Section 6, with criteria based on the 2-sigma uncertainty. QA results should be within these criteria, but tolerance depends in part on the precision and accuracy demanded of the system.

When purchasing a new LD system, all aspects should be thoroughly tested in a commissioning process before it is released for clinical use. These tests may include those done during the acceptance testing of the system but typically are more in-depth and are designed to examine how the system will be used in a particular clinical setting. Recommended tests for commissioning new LD systems are presented in Tables V and VI.

As new technologies appear on the market, new tests may be appropriate and manufacturer guidelines should be followed.

For a new reader or batch of LDs, testing should be done before it is released for use. Key elements requiring testing are shown in Table II. For a new reader, in both the high-accuracy and high-efficiency modes, k_d should be established, a new $N_{D,w}$ is expected (i.e., a new calibration curve should be created), and $k_{s,i}$ should be redetermined (as described above in Table VI). For a new batch of OSLD in high-accuracy mode, or TLD in high-accuracy or high-efficiency modes, sensitivity, and linearity may change and should be fully characterized following the commissioning steps in Tables V and VI for $N_{D,w}$, $k_{s,i}$, and k_L. Other dosimeter characteristics in these tables (e.g., k_Q and k_F) should be spot checked against the values from the previous batch. For a new batch of OSLD in high-efficiency mode, the existing calibration curve (reader-dependent) and manufacturer-specified $k_{s,i}$ should be verified by irradiating at least 5% of the new dosimeters to known doses across a range of typical clinical doses. If discrepancies outside the uncertainty limits of Chapter 6 appear, the source may be either the calibration curve or the manufacturer-specified $k_{s,i}$. The physicist should investigate both possibilities.

TABLE V. Initial commissioning of a thermoluminescent dosimeter (TLD) system.

TLD reader Test	Method
Photodetector (e.g., PMT) constancy	1. Dark current reading (≤manufacturer specification) 2. Internal system-check (e.g., source light) (establish baseline value) 3. Background reading of empty planchette (establish baseline glow curve)
End-to-end	Read out 6 *standards* across the range of measured doses. Absolute dose agreement of 2/3 of detectors should be within the expected 1-sigma uncertainty from Section 6. (e.g., 2.3% or 2.8%)[a]
Annealing	3 repetitions of irradiation-read-anneal cycle to verify stability of $k_{s,i}$ through the annealing process

TL dosimeter Test	Method (high accuracy)	Method (high efficiency)
$N_{D,w}$	Establish baseline	Create calibration curve (system sensitivity over the relevant range of doses)
$k_{s,i}$ (solid forms only)	Accept dosimeters in a given range (~2–3%)	Accept dosimeters in a given range (up to 3–5%)
k_L	Establish k_L over relevant range	N/A (included in calibration curve)
k_F	Establish k_F over relevant range	Measure over a typical range of readout delays to document variation. Apply k_F if deemed clinically significant
k_Q	Establish k_Q for relevant beams	Measure a known dose for each energy/modality to document variation. Apply k_Q if deemed clinically significant

[a]These are the goals for the high-accuracy and high-efficiency environment. If this level is not achieved, the physicist should establish this uncertainty as the baseline for their process; if better accuracy is desired, guidance is available in this report.

TABLE VI. Initial commissioning of an optically stimulated luminescent dosimeters (OSLD) system.

OSLD reader Test	Method
Photodetector (e.g. PMT) constancy	1. Dark current reading (≤manufacturer specification) 2. Consistent source reading (±4%)
Precision	Use 10 OSLDs; for each, do 5 insertions into the reader with 3 or more readings per insertion (<2% coefficient of variation for the 15 readings of each dosimeter after removing effects of depletion. Higher reader precision may be desired for high-accuracy applications.)
End-to-end	Read out 6 *standards* across the range of relevant doses. Absolute dose agreement of 2/3 of detectors should be within expected 1-sigma uncertainty from Section 6. (e.g., 1.6% or 3.4%)[a]

OSL dosimeter Test	Method (high accuracy)	Method (high efficiency)
N_{DW}	Establish baseline	Create calibration curve
$k_{s,i}$	Determine for each dosimeter	N/A (accept $k_{s,i}$ provided by manufacturer)
k_L	Establish k_L over relevant dose range	N/A (included in calibration curve)
k_F	Establish k_F over relevant time range	Measure over a typical range of readout delays to document magnitude of k_F. Apply k_F if deemed clinically significant
k_d	Establish k_d over relevant number of readouts (e.g., as in Fig. 5).	Measure over a range of readouts (e.g., as in Fig. 5). Apply k_d when necessary (e.g. for constancy dosimeter) or when deemed relevant
k_Q	Establish k_Q for relevant beams	Measure a known dose for each energy/modality to document magnitude of k_Q. Apply k_Q if deemed clinically significant

[a]These are the goals for the high-accuracy and high-efficiency environment. If this level is not achieved, the physicist should establish this uncertainty as the baseline for their process; if better accuracy is desired, guidance is available in this report.

QA procedures should be performed to ensure the continued functionality of the system as described in Tables VII and VIII. Large changes in the reader sensitivity compared to expected or observed day-to-day variability (for example, in excess of 30% for TLDs or 5% for OSLDs (see Fig. 6) but values will depend on the reader) should motivate QA of the reading environment (e.g., ensuring the nitrogen is turned on). In general, the operator should know the approximate expected signal from a particular reading.

TABLE VII. Per-session and annual quality assurance for TLD systems

Test		
Per-session QA		
Dosimeter functionality	Inspect for visible damage	
Planchette	Inspect planchette for physical damage (scratched/dented)	
Reader sensitivity	Document reader sensitivity (e.g., based on *standards*). Look for major changes	
Annealing consistency	Verify annealing temperature and times agree with annealing protocol	
	High accuracy	High efficiency
Reader performance	1. Dark current reading (≤manufacturer specification) 2. Background reading of empty planchette (no gross deviations from baseline glow curve) 3. Coefficient of variation of *standards* is less than 2%	1. Dark current reading (≤manufacturer specification) 2. Background reading of empty planchette (no gross deviations from baseline glow curve)
Test	Method (high accuracy)	Method (high efficiency)
Annual QA		
Reader sensitivity	Evaluate reader sensitivity trends	Evaluate reader sensitivity trends
Planchette	Inspect/polish	Inspect/polish

TABLE VIII. Per-session and annual quality assurance for OSLD systems.

Per-session QA Test	Method	
Dosimeter functionality	Inspect for visible damage	
Reader sensitivity	Document reader sensitivity (e.g., based on *standards*). Look for major changes	
Precision	Evaluate the coefficient of variation of a dosimeter (e.g., first dosimeter in session) over multiple (≥3) readings. Should be <2% (depletion can be corrected for if desired). The first reading may be discarded (Section 4.A)	
Bleaching verification (if applicable)	Read a subset of dosimeters (at least 5% of sample) to ensure signal is ~background	
	High accuracy	High efficiency
Reader performance	1. Dark current reading (≤manufacturer specification) 2. Consistency of reader system (relationship between dose and signal) versus previous reading sessions[a]	1. Dark current reading (≤manufacturer specification) 2. Appropriateness of calibration curve: Single reading of constancy dosimeter, reused and corrected for depletion and fading[b] (±3%)
Annual QA Test	Method: high accuracy	Method: high efficiency
Reader performance	None (system and calibration verification done every session)	Read out 6 *standards* across the range of relevant doses. Absolute dose agreement of 2/3 of detectors should be within expected uncertainty (from Section 6. e.g., 1.6% or 3.4%)[c]
Constancy	N/A (System and calibration verification done every session)	Create new constancy dosimeter
Reader sensitivity	Evaluate reader sensitivity trends	Evaluate reader sensitivity trends

[a]Dramatic deviations compared to reader performance history may indicate and underlying issue that should be investigated.
[b]Fading for constancy dosimeter can be estimated from Section 4 and/or Fig. 8(b) for the year of its use.
[c]These are the goals for the high-accuracy and high-efficiency environment. If this level is not achieved, the physicist should establish this uncertainty as the baseline for their process; if better accuracy is desired, guidance is available in this report.

8. GENERAL HANDLING

The accuracy and precision of an LD system can be substantially affected by handling techniques[73] and the uncertainty in these dosimeters can be substantially reduced when meticulous care is used in their handling, irradiation, and reading.

8.A. TLD

When dealing with solid TLDs, vacuum tweezers are ideal.[74] However, soft-tip or plastic tweezers should at a minimum be used, rather than fingers (oils from the skin can contaminate the chip, causing chemoluminescence), or hard-tipped tweezers (that can scratch or chip the TLD thereby

unpredictably changing its sensitivity). When placed onto a patient, a thin plastic envelope should protect the TLD from the oils on patient's skin. When not being used, and particularly during the period of time between irradiation and readout, high temperature (such as in a hot car) should be avoided as it can affect the sensitivity and accelerate fading. In general, TLD should be stored in a climate-controlled environment. When reading out TLDs, the reader should be warmed up for at least 30 min to allow the PMT tube temperature to stabilize. The reader may be left on indefinitely to preserve stability, but the gas should not be left on when not in use. The same planchette and slot should be used for each chip reading; changes in planchette can change readings by >4%.[75] The positioning of solid TLD forms may also have an impact on the signal. Consistent orientation of microcubes in the reader improved reproducibility by about 1.5%[72]. TLD chips may be marked along the edges or in the corners with a graphite pencil, and may be cleaned by washing in alcohol. The $k_{s,i}$ of the TLD chip should be measured after marking; such markings should make <2% change (based on the experience of an Accredited Dosimetry Calibration Laboratory), but can be much more (e.g., 14%[75]). During annealing, a consistent temperature is important. The oven should be preheated and open oven racks with plenty of air circulation should be used to avoid temperature gradients.

If using TLD powder, it should be distributed in a consistent fashion on the planchette. The distribution of powder on the planchette in a reproducible manner, both centering the powder and using a consistent amount, requires substantial experience. Inexperienced handlers should expect to see an increase up to 5% or more in the uncertainty of the TLD signal compared to optimal performance (Section 6). Moderately experienced handlers should still expect to see an increase of 1–2% in their uncertainty. Solid forms are less sensitive to experience but may still have 1–2% increased uncertainty from inexperienced users because of inconsistency in orienting and positioning.

8.B. OSLD

For nanoDot™ OSLDs there is a light-tight plastic casing around the detector crystal. If the dosimeter accidentally opens and is exposed to light, the signal loss per minute is only a few percent in ambient room light[20]; a short exposure in ambient light will therefore have minimal impact on the stored signal. OSLD are nominally insensitive to temperature and can therefore be placed on a patient without dosimetric concern — no difference in signal has been noted based on the temperature of irradiation between 10 and 40°C[20] . Nevertheless, OSLDs should be stored in a climate-controlled environment to minimize the fading effects. nanoDots™ may be submerged in water, at least for reasonably short periods of time, without affecting their performance due to a Mylar coating of the active crystal and the high chemical stability of Al_2O_3 crystals.[51] The OSLD reader should be warmed up per the manufacturer's recommendations before reading or may be left on permanently to improve the stability of the PMT. A rotary knob, present in some OSLD reader models, allows the operator to mechanically position the active volume of the OSLD in the stimulation light source. According to the experience of calibration laboratories, the experience of the operator plays a surprisingly large role in terms of the reproducibility of this positioning (and therefore the signal). For reader with a rotary knob, it should be turned slowly and gently to allow for optimal positioning.[39] Inexperienced handlers should expect to see an increase of up to ~1–2% in the uncertainty of the OSLD signal (see Section 6). For any reader, the impact of operator experience should be understood and minimized if possible.

TABLE IX. The National Fire Protection Association (NFPA) and Hazardous Materials Identification System (HMIS) hazard ratings for LiF and Al_2O_3.

	Health		Fire		Reactivity		Physical
Material	NFPA	HMIS	NFPA	HMIS	NFPA	HMIS	HMIS
LiF	1	1	0	0	0	0	[a]
Al_2O_3	0	0	0	0	1	[a]	1

NFPA ratings are on scale of 0-4, with 0 being no hazard and 4 being extreme hazard.
[a]None listed.

9. SAFETY

Safety information from the material safety data sheets of LiF, $Li_2B_4O_7$, CaF_2, and BeO, indicate concern only for LiF. LiF has been shown to be toxic upon ingestion or subcutaneous implantation in animals, resulting in fluoride poisoning,[7] although the levels at which it is toxic are relatively high compared with the amount typically used in dosimetry applications. Good laboratory rules should be employed to ensure that hands, eyes, and food and drink are not contaminated with phosphor powder and to minimize the creation and scatter of dust. Particularly when using powder, food and drink should not be present. Gloves or hand-washing facilities should be available. When powder is used, gloves have been observed to produce static with an associated risk of spreading TLD powder and should therefore be used with caution.

There is no indication that Al_2O_3 or the binding foils and plastic casing of nanoDot™ LDs pose any biological harm. BeO is extremely toxic in powder form if inhaled but is very stable in ceramic form.

The National Fire Protection Association (NFPA) and Hazardous Materials Identification System (HMIS) hazard ratings for LiF and Al_2O_3 are provided in Table IX below.

First aid measures for Al_2O_3 include (a) if inhaled, move to fresh air; (b) if skin contact occurs, wash with soap and water; (c) if eye contact occurs, flush eyes with water; and (d) if swallowed, rinse mouth with water. First aid measures for LiF include (a) if inhaled, move to fresh air and call a physician; (b) if skin contact occurs, flush skin with water; (c) if eye contact occurs, flush eyes with water for at least 15 min

and call a physician; and (d) if swallowed, induce vomiting immediately as directed by medical personnel.

10. REUSE

An advantage of LDs is that they can be reused after removing the original signal. Care is required to preserve dosimeter characteristics, and this may not be possible for extensive reuse of OSLD. There are two possibilities for reusing the LD detectors:

aThe signal can be erased by heating the crystal, that is, *annealing*, which is the standard procedure for TLDs; however, annealing is not applicable to OSLDs encapsulated in plastic because of damage to the plastic.
bFor OSLDs, the signal can be erased by exposing the detectors to light, that is, *bleaching*, which is the standard procedure for OSLDs.

10.A. Annealing TLDs

Annealing releases all trapped electrons, removing stored signal in the detector. However, annealing (before or after irradiation) also affects the glow curve and sensitivity of the detector. To maintain the same sensitivities for the detectors, it is critical to follow a consistent annealing procedure. The general consensus on the optimal annealing procedure for LiF,Mg,Ti is to anneal for 1 h at 400°C followed by 16–24 h at 80°C,[3] although shorter annealing periods may suffice[76,77] The high-temperature component eliminates the previous dose information while the low-temperature component restores the original shape of the glow curve thus maintaining the sensitivity of the TLD. With careful annealing, the sensitivity of each TLD will change minimally, including both the average sensitivity of the TLDs and the relative sensitivity of each element ($k_{s,i}$). However, because sensitivity is highly dependent on the heating and cooling cycles, this is challenging to achieve. Therefore, all TLDs in a batch should be annealed together to ensure that their heating and cooling histories are all the same and therefore preserve their relative sensitivities. Otherwise, the detectors will no longer behave as a single uniform group.

As long as the TLDs are not damaged, a consistent annealing procedure can be repeated an indefinite number of times. While a reported change of approximately 5–10% in their relative sensitivity has been reported,[6,78] experience has shown that superior preservation of relative sensitivity is achievable.

To implement an annealing program, QA of the process is important (Section 7). First, the consistency of $k_{s,i}$ (or the preservation of all TLD within the desired sensitivity window) should be verified through at least three cycles of irradiation, read out, and annealing when commissioning a new batch of TLDs or a new annealing protocol. Second, for any annealing process, the time and temperature should be monitored to ensure it follows the annealing protocol.

10.B. Bleaching OSLDs

Bleaching also removes signal from the detector, but is done with light. Bleaching can be done with a wide range of light sources; light with longer wavelengths may be less effective at erasing the OSL signal because the energy is not sufficient to release trapped signal, whereas light with shorter wavelengths may have sufficient energy to induce other effects (e.g., photoionization of defects or phototransfer of charges from deep traps to the main dosimetric traps responsible for the OSL signal, in both cases inducing an OSL signal instead of erasing it).[79] In the case of Al_2O_3:C detectors, numerous light sources have been used, including fluorescent room lights, LEDs, and tungsten halogen lamps.[1,12,20,43,51] The amount of time required for bleaching depends largely upon the light source, although 12 h is generally sufficient to reduce residual signal to background levels.

Simplistically, OSLD have several depths of traps. They have shallow traps (that spontaneously empty during the first 8 min after irradiation), dosimetric traps that are partially emptied during readout, and deep traps that require substantial energy to empty. Bleaching can effectively empty the main dosimetric traps responsible for the OSL signal, but cannot empty deep traps (that are only emptied at >600°C[80]). Because these deep traps act as competitors in the OSL process, their state of occupancy can affect the relative trapping and recombination efficiency, causing the detector's sensitivity to change with dose history. Because bleaching does not fully reset OSLDs to their preirradiated condition (it does not empty the deep traps), the accumulated dose in OSLDs affects both the sensitivity and the supralinearity (k_L) of the detectors.[20,21,39] The changes in sensitivity depend on the bleaching time, wavelength spectrum of the bleaching light source, OSLD read time, stimulation wavelength, and accumulated dose.[43] In general, bleaching approaches and associated results have been varied in the literature, and no consensus bleaching protocol has yet been developed. Results have consistently shown that sensitivity changes, but at variable accumulated dose histories and even in variable directions. Broadly, dosimeter sensitivity changes measurably (by ~±2%) somewhere after 10 Gy of accumulated dose. By 20 Gy the sensitivity changes rapidly and dramatically.[39,43] At present, published data support using these dosimeters to a maximum accumulated dose of ~10 Gy. It is recommended against using these dosimeters at greater accumulated doses in large part because of the poorly understood changes in sensitivity and supralinearity; further studies on this issue are warranted.

Rather than bleaching OSLDs, one can in principle reuse these detectors by calculating the incremental change in OSL signal since the last readout. This calculation can be done provided that the signal depletion and fading are both known and accounted for. However, this method has been shown to be less accurate than bleaching and is therefore not recommended.[39] Rather, if OSLDs are to be reused, they should be bleached after each irradiation. Given the currently finite lifespan of OSLD, tracking dose history can be one of the

greatest logistical challenges of running an OSLD program designed to reuse dosimeters.

To implement a bleaching program for OSLD, minimal QA is required because the characteristics of the detectors do not notably change over the first 10 Gy of accumulated dose. After bleaching is completed, 5% of detectors should be read to ensure that the residual signal is approximately background (Section 7).

11. SPECIFIC APPLICATIONS

11.A. External photon beams

11.A.1. Primary beam dosimetry

Primary beam applications of LDs include *in vivo* monitoring of radiotherapy delivery, use in anthropomorphic phantoms to evaluate internal organ doses, and as verification of beam calibration with an independent dosimeter. If the detector is placed bare on the patient surface (except for a protective barrier, such as a plastic envelope, to keep oils off the dosimeter), the detector measures the dose in a high-gradient region. Although this approach can yield good agreement (within 3%) between measured and calculated doses[71] it requires very attentive beam modeling in the buildup region based on high quality superficial measurements. Alternately, bolus or buildup caps can be used to move the LD into a lower-gradient region (≥5 mm depth) that will typically yield a more accurate comparison with the treatment planning system calculation. The lateral dimension of the bolus should provide for lateral charge particle equilibrium (e.g., 5 cm × 5 cm square bolus).[70]

As *in vivo* dosimeters, LDs have been shown to provide reasonable accuracy and precision. As conditions become more complicated or less tightly controlled, uncertainty in the measurements increases. In phantom measurements [using 3D and IMRT treatments], Zhuang and Olch[71] achieved agreement typically within ±3% between measurement and TPS calculation using a high-accuracy OSLD technique and a carefully tailored TPS beam model. This precision is consistent with the optimal precision shown in Table III for high-accuracy use of this detector in a "less controlled" setting. IAEA led efforts[73] for *in vivo* patient measurements using TLD and OSLD showed a spread of ±3.4% for TLD measurements and ±3.3% for OSLD (1-sigma); these approaches used a lower precision approach to managing the dosimeters, but were limited to conventional therapy, most often with Co-60 beams. In contrast to these studies run entirely by physicists, Riegel et al.[70] highlighted their experience with over 11 000 *in vivo* patient measurements implemented as part of a routine clinical workflow. OSLD were handled in a high-efficiency framework and placed by a therapist. Although their average measured-to-TPS calculated result was highly accurate, the standard deviation was 10.3%, highlighting the substantial additional uncertainty that can be introduced in a routine clinical setting. The uncertainty was higher for IMRT (11.9%) and VMAT (13.4%) than for 3D (10.5%) or field-in-field techniques (7.2%), highlighting that dosimeter placement is more of challenge for more complex therapies, but also that relatively large uncertainties exist even for simple 3D treatments.

11.A.2. Skin dosimetry

The accurate measurement of dose to the skin (or otherwise at or very near the surface) is a serious challenge. A depth of only 0.07 mm is recommended for the most superficial skin layers,[81] which greatly limits the detectors that can be used for these measurements.

A number of studies have demonstrated the use of TLDs to measure skin doses or surface doses, which typically requires extrapolation of the signal because of the relatively thick size of the dosimeter compared to the dose gradient[82–86] The relatively high density of TLDs means that the effective point of measurement is downstream from the middle of the detector compared with an equal thickness of water;[87] because the percent depth dose is so steep close to the surface, even thin TLDs can overestimate the surface dose by 10–40%.[88,89] One technique for overcoming this is to make measurements with detectors of different thicknesses, and extrapolate to the dose at the desired depth.[85,90,91]. nanoDot™ OSLDs have an effective point of measurement that is 0.8 mm deep[71] and therefore these OSLDs also substantially overestimate the surface/skin dose. The magnitude of this overestimate can exceed 50%[88] but, as with the TLD measurements, this error will depend on the treatment field and beam energy. When the surface dose is relatively high (e.g., from a large treatment field), the gradient at the surface is relatively low, so the error introduced by these dosimeters is smaller.

11.A.3. Small-field dosimetry

LDs can be suitable detectors for small field applications. TLD show very little (<1%) perturbation effect due to the nonwater equivalence of the detector material, and relatively little volume averaging effects depending on the size of the TLD used.[92] LiF microcube TLDs, which measure only 1 mm on each side,[93–95] are generally the best suited detector for these applications as they exhibit a partial volume effect of only ~0.3% even for 6 mm × 6 mm fields.[92] Overall small field correction factors for TLD microcubes have been found to be <~2% even for 4-mm circular apertures.[96–98] Microcubes have therefore been used for relative dosimetry of radiosurgery beams.[99–107] In general, TLD measurements agree with other accurate dosimetry techniques to within 2%, although measurements in fields <1 cm are challenging and often larger disagreements of 4–5% are noted.[94,100–102,105]

Larger dimension TLD can be used as well, although chips measuring 3.2 mm on a side exhibit a partial volume effect of nearly 3% for 6 mm × 6 mm fields.[92] Larger TLD in powder form (cylindrical volume 4 mm in length and 2.5 mm in diameter) have also been successfully implemented in the anthropomorphic stereotactic head phantom developed by IROC Houston[107] which uses a 1.9 cm target.

While TLDs can be used for small-field dosimetry, their use is laborious when characterizing the dosimetry for an entire set of radiosurgery field sizes and depths. TLDs are most useful for spot-checking various points in the measurement set.

Owing to the relatively large diameter of the nanoDot™ disk, small-field dosimetric measurements are more challenging and would likely be associated with notably increased uncertainty for field sizes smaller than 2 cm × 2 cm. Exploration has been done to reduce the size of the active area of the nanoDot™, thereby making it suitable for dosimetry down to 1 cm × 1 cm, but further development is required.[108] Such small field applications suffer from additional challenges in that for fields smaller than an 18-mm cone, air gaps in the dosimeter (as are present in the nanoDot™) impact the electronic equilibrium and affect the measurement by several percent.[109] It is also important to remember for these applications that the dosimeter is positioned off-center in the plastic casing.

An alternate development relevant to small field applications with OSLD is the feasibility of OSL films, which may provide the precision of OSLD combined with two-dimensional planar information.[110,111] However, further development and evaluation is still required.

11.B. Electron beams

Clinical electron measurements include total skin electron therapy, small-field irradiation, surface dose verification, extended SSD situations, oblique incidence dose verification, and evaluation of the effectiveness of a beam spoiler. Investigations into the angular dependency of low-energy electron measurements for OSLD nanoDots™ have yet to be examined, although the magnitude of this effect is likely small as it is for x-ray beams. For small electron field irradiation, the measurement is highly sensitive to the position of the LD, the active volume of which should be carefully aligned to the field. The use of OSLD nanoDots™ in particular is not recommended for electron fields smaller than 2 cm × 2 cm.

Energy dependence for electron beams is relatively small. Variations in the ratio of collisional stopping power of LD materials vs water are much smaller than variations in mass attenuation coefficients.[58] As a result, variations in dosimeter response are small for different electron energies, particularly from 1 to 20 MeV.[20,51,112] In the megavoltage range, the impact of beam quality should have a discernible effect only when the desired accuracy is better than 2.5% or under specific conditions. At kV energies, TLD-100 and nanoDots™ have decreased response to low-energy (end of range) electrons, which can lead to a measurable decrease in response, particularly at the tail of low-energy electron beams (e.g., 6 or 9 MeV).[113]

Surface dose measurements are less problematic for electron beams than for photon beams because the much less steep PDD at the surface for electron beams makes the measurement less sensitive to measurement depth variations. In particular, for total skin electron therapy[114] which uses additional scattering of the electron beam near the patient, there is little buildup of the dose at the patient surface. LDs on the patient surface therefore represent the dose to the skin with reasonable accuracy.

Patients are often treated with both electron and photon fields. As discussed in Section 4.C.3, there is a difference in response (k_Q) for both nanoDots™ and TLD-100 between these two modalities (by about 2%). Unless the different modalities can be separately measured and analyzed, additional uncertainty (of a few percent) will be introduced into a single combined measurement.[115]

11.C. Proton and ion beams

For LDs, the dosimeter response is slightly different in high-LET beams than in low-LET ones. Energy deposition from heavy charged particles is very concentrated around the particle track, creating regions of high ionization density that can exceed saturation, particularly of OSLD traps, on a microscopic scale.[116] As a result, the signal per dose deposited by high-LET radiations can be less than that with low-LET radiation, and decreasing as LET increases.[80] In proton beams, the response is around 7% higher for TLD-100 relative to 6 MV, while it is about 4% lower than at 6 MV for nanoDot™ OSLD (at ~1 Gy).[51]

There are additional subtleties to this LET effect. First, this LET effect is also dependent on fluence: as the fluence increases, particle tracks interact giving rise to nonlinearity in the dose response.[117,118] Second, the local supralinearity that drives k_Q for high-LET beams is dependent on LET: the onset of supralinearity occurs at higher doses as the LET increases.[117] Fortunately, these two effects have relatively small impacts. If one is measuring in a proton beam, the variation in LET is relatively small (except in the fall-off region beyond the bragg peak), and consequently there is little change in signal as a function of nominal proton energy[51,119,120] except on the distal side of the Bragg peak.[118] Therefore, between different proton beams, additional k_Q corrections are small and likely unnecessary. However, a significant difference in k_Q would be expected between a proton beam and a carbon beam, and even exist within a given carbon beam because of their greater LET variability.[51,121] Heavy ion beams, in particular, pose a major challenge for luminescence dosimetry. Detector responses have been found to vary not only as a function of LET, but also as a function of the ion species at a given LET. That is, different ions with the same LET yield a different response in the detector.[122] This is particularly relevant for clinical carbon beams because, except near the surface, they contain a dramatic mix of different ion species.[123]

Nonlinearity effects are less pronounced in proton beams, being only a few percent between 1 and 10 Gy, rather than ~10% over this dose range in a photon beam.[51,119] A different linearity correction or calibration curve is therefore needed for proton applications. No angular dependence was noted for OSLD (within 0.5%) in the SOBP of a 200 MeV clinical proton beam.[64]

Measurements in the distal fall-off portion of the Bragg peak suffer from several complications. First, this is a region of very sharp dose gradient and will therefore be subject to large positioning uncertainty. Moreover, at this location, the range of the particles becomes similar to the detector thickness, leading to partial volume effects. Finally, because the LET of the particles changes most dramatically at this location, the luminescence signal emitted will be affected by variation in the LET within the detector. Although the nonuniformity in the absorbed dose can be quantified by Monte Carlo calculations, it is not trivial.[124]

Measurements on the surface of a phantom or patient are relatively straightforward because of the relatively flat dose buildup. The inherent buildup of the detector introduces less error into the dose measurement.

Small proton fields have been studied with OSLD down to a size of 2 cm × 2 cm.[119] The OSLD dose agreed well with other dosimeters even at this smallest field size, although the field non-uniformity needed to be corrected for. Because clinical proton machines are highly variable, the uniformity of small proton fields may vary between accelerators. Care should be used, and corrections may be necessary, even for 2 cm × 2 cm fields.

The different peaks in the glow curves of certain TLD materials show different sensitivities to the LET of the incident radiation. Correspondingly, the relative peak intensity can be used to measure the LET in mixed radiation fields[125,126] or heavy particle beams.[127]

11.D. Brachytherapy

The small size of LD's is one of the great advantages of these detectors for measuring brachytherapy sources. However, LDs must be handled in a uniform manner to ensure optimal precision.[128] In particular, the low energy of the sources requires careful attention: energy corrections for LDs can be substantial (see Section 4.C.3), and attenuation of the beam across the thickness of the detector can manifest. Precision and uncertainty of LDs has been explored extensively for brachytherapy applications, with TG-138 elaborating on the results.[129]

TLDs have been used for patient measurements during brachytherapy, including *in vivo* measurements in the urethra and/or rectum,[130–132] as well as measurements on the skin.[133] However, the bulk of TLD use has related to verification of air kerma strength and measurement of other source parameters of the TG-43 formalism. TLD have been used to measure the radial dose function, $g(r)$, and the anisotropy function, $F(r,\theta)$, of various sources.[134] The use of TLD for brachytherapy have been given in a number of publications; the last review was in the most recent update of the TG-43 report.[135] In these studies it was possible to achieve an uncertainty of 2.2% (1-sigma), yielding a precise result. In general though, greater uncertainties are associated with non-external beam applications.[129] Of particular note, for measurements near the source, the dose gradient is substantial and can make sizeable contributions to the uncertainty. At 1 cm from the source, a 0.2-mm positioning uncertainty results in a 4% uncertainty in the delivered dose, so tight positioning tolerances are required, and increased uncertainty (compared with that in Table IV) is unavoidable for this type of measurement.

The relatively low-energy sources in brachytherapy requires detailed consideration of the energy correction required to relate the experimental and calibration conditions. This correction can be substantial: even for ^{192}Ir, TLD-100 over-responds relative to a 6 MV beam by ~5%.[46,136–138] The energy response of TLD to a variety of different sources and radionuclides have recently been published.[139,140] In addition to the generally elevated response, it is also important to consider that the spectrum around a brachytherapy source changes with penetration through material: the primary spectrum is hardened, but offsetting this is a buildup of scattered photons. This change in spectrum can have a very notable impact on the energy response, even for high-energy brachytherapy sources such as ^{192}Ir.[136,138,141] For practical measurements in a phantom, the scatter and spectrum can also be impacted by the size of the phantom[142] and the phantom composition material.[143] All of these factors contribute to variations in the k_Q associated with TLD; minimizing differences between reference and experimental conditions will help minimize the size and impact of these variations. As part of k_Q, it must also be remembered that TLD have an intrinsic energy response that is not captured by Monte Carlo simulations, requiring that the energy dependence be empirically determined. Such empirical determinations have been reported recently based on measurements in a calibrated kV x-ray source.[139,144] These empirical determinations have then been verified for brachytherapy sources including ^{125}I, ^{103}Pd, and ^{192}Ir.[137,145]

A second consideration associated with low-energy brachytherapy sources is self-absorption of the beam by the crystal itself. This produces a nonuniform irradiation of the crystal and an apparent under-response (see Fig. 9). The magnitude of this effect will depend on the size and shape of TLD.[145] It will also manifest as an angular dependence as the effect will be more pronounced for longer paths through the TLD. In general for such scenarios, the thinner the LD, the greater the accuracy of the measurement.[146]

A good summary reference for the use of OSLD in brachytherapy is given in the OSLD section of the AAPM summer school report.[9] Recent investigations have been done measuring doses in high-dose rate brachytherapy environments with OSLDs.[66,147,148] As with TLD, the steep dose gradients mean that measurements are very sensitive to setup error. Beam quality dependence is also a major consideration as the effects are more pronounced than for TLD. When measuring dose from ^{192}Ir, OSLDs have been calibrated in cobalt[147] (requiring ~6% correction compared to ^{60}Co) and with an ^{192}Ir source[66] and both have worked successfully. However, regardless of calibration approach, there can be substantial spectral variation as a function of distance from the source. That is, k_Q varies as more material separates the source and detector. This effect was nearly 10% between 2 and 10 cm of solid water for ^{192}Ir.[66] Additionally, the

different filtration of different sources can also lead to different k_Q factors: Nucletron and Varian Ir-192 sources were found to have different energy responses by 2.6%.[147] An angular dependence of ~4% between edge-on and en-face irradiations of the nanoDot™ LD has been observed in ^{192}Ir because of asymmetric attenuation of the beam in the plastic casing and across the OSLD disk itself.[66] As a final note, it has been observed[66] that the sensitivity changes observed after large accumulated doses (>10 Gy) are not consistent between megavoltage energy and ^{192}Ir, further justifying the 10 Gy accumulated dose limit for nanoDot™ LDs.

Other low-energy therapeutic applications, such as measuring doses from orthovoltage or animal irradiators, require similar considerations in terms of managing beam quality and angular dependence corrections.

Calibration of LDs in a brachytherapy setting can either be done with the brachytherapy source (in which case the beam quality dependence is small, but the absolute calibration dose is more uncertain) or with a megavoltage source (in which case the absolute calibration dose is highly certain but a larger beam quality correction is necessary). Both approaches have been successful, but Haworth et al.[149] found superior results using a brachytherapy-based calibration.

11.E. Imaging

Thermoluminescent dosimeters and OSLDs are useful dosimeters for imaging applications, as they have high sensitivity and can generally measure low doses with good accuracy. The general formalisms described in this report for both TLDs and OSLDs can be applied for kilovoltage applications. However, several considerations are warranted.

Overviews of LD characteristics (particularly for the nanoDot™) have been recently published for kV environments.[44,150] Applications of these detectors have included CT, where studies have measured doses during diagnostic examinations,[151] cone-beam CT procedures as part of an image-guided radiotherapy,[152,153] CT dose index,[154] and mail-based audits.[155] Skin dose assessment during fluoroscopic-guided and CT-fluoroscopic-guided interventional procedures has also been done using both TLD and OSLD,[156–160] as has measuring dose in mammography.[44,155]

The first consideration is determining the calibration factor ($N_{D,w}$) for *standards* associated with an imaging application. Calibrations are most often performed in the kV environment using a typical beam and cross calibrating the LD vs ionization chamber measurements.[156,157,159] A challenge of this approach is in determining the reference dose to the *standards* (D_0), which typically has higher uncertainty than that associated with therapeutic applications. Alternatively, calibration may be performed in a therapy environment, which will be associated with higher precision in the dose to the *standards* (D_0), but will require the application of a large k_Q correction to the experimental dosimeters (Fig. 9). A final calibration approach exists for some dosimetry systems, where the calibration coefficient is offered by the manufacturer. For OSLD in a CT setting, the first two options were found to provide comparable uncertainty (within 5% at the 1-sigma level using a high-accuracy approach) while the manufacturer-based calibration had an average uncertainty in excess of 15%.[161]

A major challenge is the energy dependence of the dosimeter, which is substantial and highly variable for TLD and OSLD in the energy range of imaging applications. Being highly sensitive to the beam energy not only introduces a large uncertainty, it also requires a good understanding of the underlying spectra at the exact point of measurement (usually requiring Monte Carlo simulations). For kV photons, TLDs over-respond by a factor of up to 1.4[52,162] relative to ^{60}Co. Of note, this beam quality dependence can vary with different sizes and shapes of TLD[145]. The magnitude of over-response to low-energy beams is much greater for OSLDs, which over-respond by a factor of as much as 3 to 4 relative to ^{60}Co.[21,41,44,51,59,163–166] If the calibration is done in a kV environment, the beam quality correction factor will be less. However, a beam quality correction factor may still be substantial (particularly for OSLDs) between the calibration and experimental irradiation conditions as the energy response changes substantially even with small changes in beam quality in the kV energy range. Selection of kV (e.g., 140 kVp vs 80 kVp) affects k_Q by approximately ±10–15%.[41,44,150,153] Presence of a bow-tie filter and the presence and thickness of material in the beam can also impact k_Q by approximately ±10% each.[41,150,152,153] Even different amounts of scatter arising from different scan extents in a CT setting had a measurable impact on k_Q (<4%).[41] The variation in energy dependence of LDs in imaging environments, particularly those other than CT, would benefit from further quantification.

Angular dependence may also play a sizeable role at kV energies, at least for the nanoDot™. Relative to en-face irradiation of the nanoDot™ disk, irradiation of the edge resulted in 20–30% less measured dose in radiography and 60% less measured dose in mammography.[44] In computed tomography, the issue is further complicated because of the rotation of the source. Angular dependences of 10–20% has been observed in air [41,150] but for measurements done in a phantom, the angular dependence is <5% (both for en-face vs rotating irradiation and for the CT scanner rotating around different orientations of the dosimeter).[41,150] This has not generally been observed as an issue for TLD, largely because TLD forms are typically more symmetric, but at very low energies (e.g., mammography) TLD orientation can also result in variations in absorption in the crystal, manifesting as angular dependence. Angular dependence in clinical procedures (e.g., fluoroscopy-guided interventions) may be particularly difficult to manage because not only will there be an angle of the dosimeter on the patient's skin, the beam may also be incident from different directions. Fully accounting for this would likely be impossible, resulting in increased uncertainty in the final dose estimate.

Self-attenuation of LDs also becomes an issue at very low energies (e.g., in mammography). Attenuation of the beam by the detector becomes a substantial effect that requires careful consideration.[48,167] nanoDot™ OSLDs are thin and therefore self-attenuation in an en-face irradiation configuration is minimized and has not been identified as being of concern.

Supralinearity in LDs is generally not a concern because the doses are typically much lower in kV environments than in MV environments. k_L has been found to be unity up to ~1 Gy for nanoDot™ LDs[150] and generally even higher for TLD. For nanoDot™ use, if the low-dose setting is used on the reader, the operator should ensure that the reader is not saturated if relatively high doses are read. On the other hand, for very low doses, the reading may be obscured by noise. Although relatively precise measurements can be made at doses as low as 5 mGy[41] nanoDot™ LDs in particular will show background signals that will depend on the reader used and the bleaching procedure for the dot. If a low dose is expected, the background signal of the dosimeter should be evaluated.

If the kV irradiation is part of an image-guided radiation therapy setting, it is usually of interest to know both the imaging dose and the therapeutic dose. However, because of the different beam qualities and the inability to distinguish the sources of dose, it is not reasonable to get both kV and MV doses at the same time; different dosimeters with different calibrations and/or corrections would be needed to identify each dose component.

11.F. Out-of-field applications

LDs are a popular option for out-of-field dose measurements because of their high sensitivity and small size.[168] These measurements include *in vivo* patient monitoring (e.g., fetal or pacemaker dose assessments) as well as measurements in phantoms. Such measurements require particular attention to several details.

First, the energy of the out-of-field spectrum is considerably lower than that inside the treatment field,[52,61] resulting in an over-response of the detector calibrated in-field. At 6 MV, TLD-100 over-responds by 4–12%[52] increasing with greater distances from the field edge. For nanoDot™ OSLDs, the over-response ranges from 10% to 25%.[53]

Second, a detector placed on the patient's surface is often intended to be a measure of the dose at depth. However, outside the treatment field, the dose is elevated at depths shallower than d_{max} (by a factor of as much as 5 compared with the dose at d_{max}). At any depth deeper than d_{max}, the dose is approximately constant with depth. Therefore, unless the superficial dose is of interest, bolus should be placed over the LD when making out-of-field measurements. Failure to do so may cause an overestimation of dose by a factor of up to 5. The bolus thickness should be at least similar to the d_{max} thickness of the nominal beam.[169–171]

Third, caution may be warranted if doses are being measured in an image-guided radiation therapy environment if the dosimeter is outside the primary photon field but within the imaging field. Both these procedures may deliver comparable dose, but due to the high atomic number of most LDs, particularly for nanoDot™ OSLDs, the signal from the imaging procedure may artificially dominate.

Finally, the presence of neutrons must be considered during irradiation using photon beams with energy >10 MV. In particular, TLD-100 substantially over-responds to neutrons. Although this effect is negligible inside the treatment field (due to dominance of photons), outside the treatment field, TLD-100 over-responds and can provide a dose estimate in error by a factor of more than 10 because of neutron contamination.[172] Thus, TLD-100 should not be used outside the treatment field for energies >10 MV. Instead, a neutron-insensitive dosimeter should be used to assess the gamma component of the dose, followed by a separate assessment of the neutron component. This requires dosimeters that are insensitive to neutrons such as TLD-700. Al_2O_3:C also has a very low response to neutrons,[173] although the impact of the plastic casing has not yet been thoroughly evaluated.

11.G. Measurement of secondary neutrons

High-energy (>10 MV) photon radiotherapy includes secondary neutrons. Neutron detection by TLDs in a mixed -n field requires two different types of TL materials: one sensitive to both photons and neutrons and the other sensitive only to photons.[174] The neutron component can then be determined by the difference between the responses of the two materials. The TLDs most commonly used for these types of measurements are TLD-600 (95.62% of the lithium is ^{6}Li) and TLD-700 (99.93% of the lithium is ^{7}Li).

The neutron interaction cross-section for different lithium isotopes is a complicated function of energy but is a maximum for thermal neutrons. TLD-600 has a thermal neutron cross-section that is >1000 times as large as that of TLD-700[175] and is therefore a sensitive thermal neutron detector, whereas the TLD-700 response is essentially limited to the photon component only. Neither type of TLD is typically useful for measuring neutrons with energy above thermal. Because TLDs are only thermal neutron detectors, TLD-600 or TLD-600/TLD-700 pairs must be used in conjunction with a neutron moderator — for example, a Bonner sphere.[176–180] The response of the detectors within the moderator requires a detailed calibration (see Ref. [181]) that relates signal (thermal neutron fluence) to neutron dose or dose equivalent. This calibration relationship cannot be generally applied to arbitrary conditions, for example, a calibration in air cannot be applied to a measurement on the surface of a patient or inside a phantom. The relative quantities of thermal neutrons (what is measured) vs fast neutrons (which deposit the dose) changes drastically within the patient or under different conditions.[182] This means that the calibration relationship changes, and changes substantially, with position. More details and possible solutions are discussed in the AAPM TG-158 report, but great caution should be employed when conducting neutron measurements with LDs.[23]

Analogous to TLD-600/TLD-700 pairs, neutron-sensitive OSLDs (OSLNs) and regular OSLDs (which are neutron

insensitive) can be used for neutron dosimetry in mixed neutron/gamma fields. OSLNs, based on Al_2O_3:C, are available commercially.[183,184] These detectors are produced using a composite of Al_2O_3:C powder and a neutron converter: lithium carbonate enriched with ^{6}Li ($^6Li_2CO_3$). The neutron capture reaction with ^{6}Li generates charged particles (^{4}He and ^{3}H) that deposit energy in the Al_2O_3:C and generate an OSL signal. The neutron sensitivity in OSLNs is due to the neutron capture reaction with ^{6}Li. OSLNs are therefore only thermal neutron detectors, and as such are subject to the same substantial complications in relating thermal neutron signal to fast neutron dose.[23]

11.H. Intraoperative therapy

Unique considerations for intraoperative therapy are proper sterilization[185] of the devices and biocompatibility. Critical items are most often sterilized with steam sterilization involving high temperatures. Heat sterilization is *not* appropriate for LDs owing to their heat sensitivity. For OSLDs, heat could also damage the plastic casing, and liquid sterilization could damage the bar code. These problems can be overcome by sealing the dosimeter in a Mylar bag and then sterilizing it with ethylene oxide or Sterad. Biocompatibility is not a problem if the detectors are properly isolated from the patient, for example, packaged in a Mylar bag. However, there may be minor concern if the packaging breaks open (Section 9).

11.I. Interface dosimetry

There are many interfaces in patient anatomy where dosimetry may be relevant. The most obvious scenario is at the patient surface, where the dose to the skin is of clear clinical concern (Section 11.A.2). However, special considerations are warranted for more general evaluations of interfaces; this is most pronounced for interfaces with relatively high-Z materials, including bone as well as metal implants, and for beams of low energy such as kV x rays.

The amount of backscatter or forward scatter associated with an interface, manifesting as a spike in the dose near the interface, is often the quantity of interest. The effect can both substantial in magnitude and occurs over a very short distance. As such, it represents a very steep dose gradient. The effective point of measurement is therefore critical to consider. For TLD, the effective point of measurement depends on the thickness of the crystal used. The depth dimension of the TLD should be scaled by the electron density (e-/cm^3), which is 7.34×10^{23} cm^{-3} and 2.2 times that of water for TLD-100.[186] To measure the dose directly at the interface, crystals of varying thickness can be used allowing for extrapolation to zero detector thickness.[85,187] TLD crystals of various thickness are available, including standard chips with physical thickness of 0.9 mm, and extra thin TLD with a physical thickness of 0.14 mm. For OSLD nanoDots™, it is not possible to vary the thickness; the effective point of measurement is 0.8 mm downstream from the front of the detector.[71]

An added complexity, amplified with higher effective Z, is that the spectrum of the scattered radiation is not equivalent to that of the primary beam. Instead, it is comprised of low-energy fluorescence photons and low-energy electrons.[188–190] This introduces additional energy dependence into the detector response. Studies have indicated that changes in the spectrum, at least in terms of detector response, is dominated by the low-energy scattered electrons, not low-energy scattered photons.[189,190] The change in detector response is therefore being driven by changes in the relative mass stopping power ratios between the LD and water. As discussed in Section 4.C, these differences are minimal, even for low-energy electrons, so minimal impact is expected in terms of dosimeter response.

11.J. High-dose irradiators for blood and cells

The small size of these detectors makes them amenable to cellular and animal organ dose measurements. The first consideration is the high dose used, which will require appropriate dose-level calibration and corrections to account for nonlinearities in the detector response. The second consideration is that these irradiators often use low orthovoltage energies. Not only can energy corrections exceed 40% for LiF TLDs and 200% for Al_2O_3 OSLDs relative to 6 MV,[51–53] but in addition, the correction factor is very sensitive to small changes in the spectrum at these energies, particularly for OSLD. Beams of identical kVp can have very different energy correction factors due to different added filtration. The effective energy of the beams should be determined from half-value layer measurements.

TABLE X. Recommended information to be included when reporting thermoluminescent dosimeter (TLD) or optically stimulated luminescent dosimeter (OSLD) results.

Item	Details to include
Detector	• Material, commercial name, manufacturer • Detector physical form and dimensions • Detector selection methodology (i.e., pre-selection, $k_{s,i}$ window, individual $k_{s,i}$)
Readout	TLD and OSLD • Reader type, model, manufacturer • Number of detectors used • Dose calculation formalism • Any corrections applied and how they were evaluated TLD • Maximum readout temperature OSLD • Number of readouts for each detector
Calibration	• Number and type of *standards* used • Radiation quality in which calibration was performed • Any corrections used in the calibration (e.g., energy dependence, supralinearity)
Uncertainty	• Typical reproducibility (at a given dose level) • Estimated uncertainties • Other relevant information

12. STANDARDIZATION OF DOSE REPORTING

When documenting an LD process, either as a clinical report or a research publication, there are several important details that should be explicitly included. Following Kron et al.[191] and Yukihara and McKeever,[21] Table X presents a checklist of items that should be reported when using TLD or OSLD.

13. RECOMMENDATIONS

General recommendations:

- Whenever starting to use a new dosimeter, a series of phantom and *in vivo* measurements comparing the old and new dosimeters should be performed as in Section 7. The precision and accuracy should be similar to that predicted by Section 6.
- Define a calibration and readout process (examples are provided in Section 6) that meets clinical needs based on workflow and acceptable uncertainty.
- Review and apply the commissioning and ongoing QA protocols (Section 7).
- Know the uncertainties associated with your chosen approach (Section 6).
- Handle LDs with care to avoid damage (Section 8).
- Use LDs (including annealing/bleaching, storage, handling, etc.) in a consistent manner to maximize reproducibility (Sections 2, 7, 8 and 10).

Dose calculation recommendations:

- Readout Reproducibility. It is recommended to average the results of at least three readouts for each OSLD (Section 4.A).
- System Calibration Coefficient ($N_{D,w}$). For TLD use, the calibration coefficient must be determined for every reading session. For OSLDs, the user may decide on the frequency of its determination, recognizing the trade-off between session-specific determination and the time and resources spent determining the calibration coefficient (Sections 4.B and 6).
- Linearity (k_L). This correction factor may be accounted for, depending on desired accuracy, via a correction factor or calibration curve. It should be minimized by irradiating *standards* to the same dose as expected for the experimental results (Sections 4.C.1 and 6).
- Fading (k_F). This may be corrected for depending on desired accuracy. The effect may be minimized by matching the wait time between irradiation and readout for the *standards* and *experimentals*. The wait time should be at least 10 min for Al_2O_3:C-based OSLDs and at least 12 h for LiF:Ti,Mg-based TLDs (Sections 4.C.2 and 6).
- Beam Quality (k_Q). Beam quality corrections are necessary when there is a discrepancy between the experimental and calibration energy spectra. Particular attention should be given to out-of-field measurements, brachytherapy, diagnostic, particle therapy, and orthovoltage measurements (Sections 4.C.3, 6 and 11.C–11.F).
- Angular Sensitivity (k_θ). For geometrically asymmetric LDs, the best practice is to preserve the orientation of the LD relative to the incoming radiation between calibration and experimental measurements. The effects of this factor are more substantial in the diagnostic energy range (Sections 4.C.4 and 6).
- Signal Depletion (k_d; OSLDs only). The user should determine the magnitude of this effect during commissioning and introduce a correction factor if the magnitude is deemed relevant (Sections 4.A and 7).
- Element Sensitivity ($k_{s,i}$) (solid LDs only). The user may determine an acceptability window or track the relative sensitivity of each LD (Sections 5 and 6).

Reuse recommendations:

- If a consistent annealing procedure is used, TLDs may be reused indefinitely (Section 10.A).
- All individual TLDs from a batch should be annealed as a group to maintain their common properties (Section 10.A).
- nanoDot™ OSLDs should be used only up to a cumulative dose of 10 Gy. Use to higher doses introduces many complications including changes in sensitivity, linearity, and background signal that are dependent on the bleaching history (Sections 4.C.1 and 10.B).

Special measurement recommendations:

- For brachytherapy applications, special attention should be paid to dose gradients and to the beam quality correction factor; angular dependence may also require attention (Section 11.D).
- For imaging applications, calibration and energy correction factors require particular attention, as may angular dependence. Additionally, the background signal may need to be monitored (Section 11.E).
- For out-of-field measurements of photons >10 MV, select an LD that is neutron insensitive to avoid detector over-response to neutron contamination (Section 11.F).
- Secondary neutron dosimetry with LD must be performed with the full understanding of the energy response of the detector. LDs only respond meaningfully to thermal neutrons (Section 11.G).

CONFLICT OF INTEREST

The authors have no conflict to disclose.

[a]Author to whom correspondence should be addressed. Electronic mail: sfkry@mdanderson.org.

REFERENCES

1. Jursinic PA. Changes in optically stimulated luminescent dosimeter (OSLD) dosimetric characteristics with accumulated dose. Medical physics 39, 5788-5788 (2012).. *Med Phys*. 2010;37:132–140.
2. Bos AJJ. High sensitivity thermoluminescence dosimetry. *Nucl Instrum Methods Phys Res B*. 2001;184:3–28.
3. Cameron JR, Suntharalingam N, Kenney GN. *Thermoluminescent Dosimetry*. Madison: University of Wisconsin Press; 1968.
4. Horowitz YS. *Thermoluminescence and Thermoluminescent Dosimetry*. Boca Raton, FL: CRC Press; 1984.
5. McKeever SWS. *Thermoluminescence of Solids*. Cambridge Cambridgeshire, New York: Cambridge University Press; 1985.
6. Oberhofer M, Scharmann A. Commission of the European Communities. Joint Research Centre. Ispra Establishment, *Applied thermoluminescence dosimetry : lectures of a course held at the Joint Research Centre, Ispra, Italy, 12–16 November 1979*. (Published for the Commission of the European Communities by A. Hilger, Bristol; 1981.
7. McKinlay AF. *Thermoluminescence Dosimetry*. Briston, UK: Adam Hilger Ltd.; 1981.
8. Bøtter-Jensen L, McKeever SWS, Wintle AG. *Optically Stimulated Luminescence Dosimetry*, 1st edn. Amsterdam, Boston, London: Elsevier; 2003.
9. Cygler JE, Yukihara EG. Optically stimulated luminescence (OSL) dosimetry in radiotherapy. In Rogers DWO, Cygler JE, eds. *Clinical Dosimetry Measurements in Radiotherapy* (AAPM 2009 Summer School), Madison, WI: Medical Physics Publishing; 2009.
10. McKeever SW. New millennium frontiers of luminescence dosimetry. *Radiat Prot Dosimetry*. 2002;100:27–32.
11. McKeever SW, Moscovitch M. On the advantages and disadvantages of optically stimulated luminescence dosimetry and thermoluminescence dosimetry. *Radiat Prot Dosimetry*. 2003;104:263–270.
12. Yukihara EG, Mardirossian G, Mirzasadeghi M, Guduru S, Ahmad S. Evaluation of Al2O3: C optically stimulated luminescence (OSL) dosimeters for passive dosimetry of high-energy photon and electron beams in radiotherapy. *Med Phys*. 2008;35:260–269.
13. Yukihara EG, McKeever SWS. *Optically Stimulated Luminescence : Fundamentals and Applications*. Chichester, West Sussex: Wiley; 2011.
14. DeWerd LA, Stoebe TG. Thermoluminescent properties of solids and their applications: thermoluminescence, used in such applications as the measurement of ionizing radiation, the dating of ancient artifacts, and in geological studies, depends upon the defect properties of solids. *Am Sci*. 1972;60:303–310.
15. DeWerd LA, Bartol LJ, Davis SD. *Thermoluminescence Dosimetry*. Madison, WI: Medical Physics Publishing; 2009.
16. Chen R, McKeever SWS. *Theory of Thermoluminescence and Related Phenomena*. Singapore, River Edge, NJ: World Scientific; 1997.
17. Chen R, Pagonis V. Thermally and optically stimulated luminescence : a simulation approach. (Wiley, The Atrium, Southern Gate, Chichester, West Sussex, UK; Hoboken, NJ); 2011.
18. Bøtter-Jensen L, Thomsen KJ, Jain M. Review of optically stimulated luminescence (OSL) instrumental developments for retrospective dosimetry. *Radiat Meas*. 2010;45:253–257.
19. Akselrod MS, McKeever SWS. A radiation dosimetry method using pulsed optically stimulated luminescence. *Radiat Prot Dosimetry*. 1999;81:167–175.
20. Jursinic PA. Characterization of optically stimulated luminescent dosimeters, OSLDs, for clinical dosimetric measurements. *Med Phys*. 2007;34:4594–4604.
21. Yukihara EG, McKeever SW. Optically stimulated luminescence (OSL) dosimetry in medicine. *Phys Med Biol*. 2008;53:R351–R379.
22. Antonio PL, Pinto TCNO, Silva RMV, Souza DN, Caldas LVE. The use of the TL and OSL phenomena for determination of absorbed dose rates of Sr-90+Y-90 sources by a postal method. *Radiat Meas*. 2014;71:305–309.
23. Kry SF, Bednarz B, Howell RM, et al. AAPM TG 158: measurement and calculation of doses outside the treated volume from external-beam radiation therapy. *Med Phys*. 2017;44:e391–e429.
24. Fernandez SD, Garcia-Salcedo R, Mendoza JG, et al. Thermoluminescent characteristics of LiF:Mg, Cu, P and CaSO4: Dy for low dose measurement. *Appl Radiat Isotopes*. 2016;111:50–55.
25. Fernandez SD, Garcia-Salcedo R, Sanchez-Guzman D, et al. Thermoluminescent dosimeters for low dose X-ray measurements. *Appl Radiat Isotopes*. 2016;107:340–345.
26. Bubula E, Byrski E, Lesiak J, Waligórski MPR. Development of TL dosimeters based on MTS-N (LiF:Mg, Ti) detectors for in vivo dosimetry in a Co-60 beam. *Rep Pract Oncol Radiother*. 1998;3:43–47.
27. Sadek AM, Khamis F, Polymeris GS, Carinou E, Kitis G. Similarities and differences between two different types of the thermoluminescence dosimeters belonging to the LiF family. *Phys Status Solidi C*. 2017;14:1600220.
28. Mckeever SWS, Moscovitch M, Townsend PD. *Thermoluminescence Dosimetry Materials Properties and Uses*. Ashford, Kent, UK: Nuclear Technology Publishing; 1995.
29. Sommer M, Jahn A, Henniger J. A new personal dosimetry system for HP(10) and HP(0.07) photon dose based on OSL-dosimetry of beryllium oxide. *Radiat Meas*. 2011;46:1818–1821.
30. Yukihara EG. Luminescence properties of BeO optically stimulated luminescence (OSL) detectors. *Radiat Meas*. 2011;46:580–587.
31. Sommer M, Henniger J. Investigation of a BeO-based optically stimulated luminescence dosemeter. *Radiat Prot Dosimetry*. 2006;119:394–397.
32. Asena A, Crowe SB, Kairn T, et al. Response variation of optically stimulated luminescence dosimeters. *Radiat Meas*. 2014;61:21–24.
33. Lehmann J, Dunn L, Lye JE, et al. Angular dependence of the response of the nanoDot OSLD system for measurements at depth in clinical megavoltage beams. *Med Phys*. 2014;41:061712.
34. Jursinic PA. Angular dependence of dose sensitivity of nanoDot optically stimulated luminescent dosimeters in different radiation geometries. *Med Phys*. 2015;42:5633–5641.
35. Bilski P. Lithium fluoride: from LiF : Mg, Ti to LiF : Mg, Cu, P. *Radiat Prot Dosimetry*. 2002;100:199–206.
36. Moscovitch M, Horowitz YS. Thermoluminescent materials for medical applications: LiF : Mg, Ti and LiF : Mg, Cu, P. *Radiat Meas*. 2006;41:S71–S77.
37. Olko P, Bilski P, Kim JL. Microdosimetric interpretation of the photon energy response of LiF : Mg, Ti detectors. *Radiat Prot Dosimetry*. 2002;100:119–122.
38. Bartolotta A, Brai M, Caputo V, et al. The response behavior of LiF-Mg, Cu, P thermoluminescence dosimeters to high-energy electron-beams used in radiotherapy. *Phys Med Biol*. 1995;40:211–220.
39. Mrcela I, Bokulic T, Izewska J, Budanec M, Frobe A, Kusic Z. Optically stimulated luminescence in vivo dosimetry for radiotherapy: physical characterization and clinical measurements in (60)Co beams. *Phys Med Biol*. 2011;56:6065–6082.
40. Almond PR, Biggs PJ, Coursey BM, et al. AAPM's TG-51 protocol for clinical reference dosimetry of high-energy photon and electron beams. *Med Phys*. 1999;26(9):1847–1870.
41. Scarboro SB, Cody D, Alvarez P, et al. Characterization of the nanoDot OSLD dosimeter in CT. *Med Phys*. 2015;42:1797–1807.
42. Dunn L, Lye J, Kenny J, Lehmann J, Williams I, Kron T. Commissioning of optically stimulated luminescence dosimeters for use in radiotherapy. *Radiat Meas*. 2013;51–52:31–39.
43. Omotayo AA, Cygler JE, Sawakuchi GO. The effect of different bleaching wavelengths on the sensitivity of Al(2)O(3): C optically stimulated luminescence detectors (OSLDs) exposed to 6 MV photon beams. *Med Phys*. 2012;39:5457–5468.
44. Al-Senan RM, Hatab MR. Characteristics of an OSLD in the diagnostic energy range. *Med Phys*. 2011;38:4396–4405.
45. Nath R, Anderson LL, Luxton G, Weaver KA, Williamson JF, Meigooni AS. Dosimetry of interstitial brachytherapy sources - recommendations of the aapm radiation-therapy committee task group no 43. *Med Phys*. 1995;22:209–234.
46. Tedgren AC, Hedman A, Grindborg JE, Carlsson GA. Response of LiF:Mg, Ti thermoluminescent dosimeters at photon energies relevant to the dosimetry of brachytherapy (< 1 MeV). *Med Phys*. 2011;38:5539–5550.
47. Karsch L, Beyreuther E, Burris-Mog T, et al. Dose rate dependence for different dosimeters and detectors: TLD, OSL, EBT films, and diamond detectors. *Med Phys*. 2012;39:2447–2455.
48. Nunn AA, Davis SD, Micka JA, DeWerd LA. LiF:Mg, Ti TLD response as a function of photon energy for moderately filtered x-ray

spectra in the range of 20–250 kVp relative to 60Co. *Med Phys*. 2008;35:1859–1869.
49. Karzmark CJ, White J, Fowler JF. Lithium fluoride thermoluminescence dosimetry. *Phys Med Biol*. 1964;16:273–286.
50. Meigooni AS, Mishra V, Panth H, Williamson J. Instrumentation and dosimeter-size artifacts in quantitative thermoluminescence dosimetry of low-dose fields. *Med Phys*. 1995;22:555–561.
51. Reft CS. The energy dependence and dose response of a commercial optically stimulated luminescent detector for kilovoltage photon, megavoltage photon, and electron, proton, and carbon beams. *Med Phys*. 2009;36:1690–1699. Erratum: 2012;39:5788.
52. Scarboro SB, Followill DS, Howell RM, Kry SF. Variations in photon energy spectra of a 6 MV beam and their impact on TLD response. *Med Phys*. 2011;38:2619–2628.
53. Scarboro SB, Followill DS, Kerns JR, White RA, Kry SF. Energy response of optically stimulated luminescent dosimeters for non-reference measurement locations in a 6 MV photon beam. *Phys Med Biol*. 2012;57:2505–2515.
54. Gasparian PBR, Vanhavere F, Yukihara EG. Evaluating the influence of experimental conditions on the photon energy response of Al2O3: C optically stimulated luminescence detectors. *Radiat Meas*. 2012;47:243–249.
55. Aznar MC, Andersen CE, Botter-Jensen L, et al. Real-time optical-fibre luminescence dosimetry for radiotherapy: physical characteristics and applications in photon beams. *Phys Med Biol*. 2004;49:1655–1669.
56. Viamonte A, da Rosa LA, Buckley LA, Cherpak A, Cygler JE. Radiotherapy dosimetry using a commercial OSL system. *Med Phys*. 2008;35:1261–1266.
57. Schembri V, Heijmen BJM. Optically stimulated luminescence (OSL) of carbon-doped aluminum oxide (Al2O3: C) for film dosimetry in radiotherapy. *Med Phys*. 2007;34:2113–2118.
58. Johns HE, Cunningham JR. *The Physics of Radiology*. Springfield Il: Charles Thomas Publishing; 1983.
59. Scarboro SB, Kry SF. Characterisation of energy response of Al(2)O (3): C optically stimulated luminescent dosemeters (OSLDs) using cavity theory. *Radiat Prot Dosimetry*. 2013;153:23–31.
60. Jang SY, Liu HH, Mohan R, Siebers JV. Variations in energy spectra and water-to-material stopping-power ratios in three-dimensional conformal and intensity-modulated photon fields. *Med Phys*. 2007;34:1388–1397.
61. Edwards CR, Mountford PJ. Near surface photon energy spectra outside a 6 MV field edge. *Phys Med Biol*. 2004;49:N293–N301.
62. Struelens L, Vanhavere F, Smans K. Experimental validation of Monte Carlo calculations with a voxelized Rando-Alderson phantom: a study on influence parameters. *Phys Med Biol*. 2008;53:5831–5844.
63. Mobit P, Badragan I. Angular and radial dependence of the energy response factor for LIF-TLD micro-rods in 125L permanent implant source. *Radiat Prot Dosimetry*. 2006;120:70–73.
64. Kerns JR, Kry SF, Sahoo N, Followill DS, Ibbott GS. Angular dependence of the nanoDot OSL dosimeter. *Med Phys*. 2011;38:3955–3962.
65. Kim DW, Chung WK, Shin DO, et al. Dose response of commercially available optically stimulated luminescent detector, Al2O3: C for megavoltage photons and electrons. *Radiat Prot Dosimetry*. 2012;149:101–108.
66. Sharma R, Jursinic PA. In vivo measurements for high dose rate brachytherapy with optically stimulated luminescent dosimeters. *Med Phys*. 2013;40:071730.
67. Kirby TH, Hanson WF, Johnston DA. Uncertainty analysis of absorbed dose calculations from thermoluminescence dosimeters. *Med Phys*. 1992;19:1427–1433.
68. Izewska J, Andreo P, Vatnitsky S, Shortt KR. The IAEA/WHO TLD postal dose quality audits for radiotherapy: a perspective of dosimetry practices at hospitals in developing countries. *Radiother Oncol*. 2003;69:91–97.
69. Alvarez P, Kry SF, Stingo F, Followill D. TLD and OSLD dosimetry systems for remote audits of radiotherapy external beam calibration. *Radiat Meas*. 2017;106:412–415.
70. Riegel AC, Chen Y, Kapur A, et al. In vivo dosimetry with optically stimulated luminescent dosimeters for conformal and intensity-modulated radiation therapy: a 2-year multicenter cohort study. *Pract Radiat Oncol*. 2017;7:E135–E144.
71. Zhuang AH, Olch AJ. Validation of OSLD and a treatment planning system for surface dose determination in IMRT treatments. *Med Phys*. 2014;41:081720.
72. da Rosa LA, Regulla DF, Fill UA. Reproducibility study of TLD-100 micro-cubes at radiotherapy dose level. *Appl Radiat Isot*. 1999;50:573–577.
73. IAEA. *International Atomic Energy Agency Development of Procedures for In Vivo Dosimetry in Radiotherapy*. Vienna: International atomic energy agency; 2013.
74. Dewerd LA. Handling technique for thermoluminescent dosimeters. *Health Phys*. 1976;31:525–526.
75. Wood JJ, Mayles WP. Factors affecting the precision of TLD dose measurements using an automatic TLD reader. *Phys Med Biol*. 1995;40:309–313.
76. Driscoll C, Barthe J, Oberhofer M. Annealing procedures for commonly used radiothermoluminescent materials. *Radiat Prot Dosimetry*. 1986;14:17–32.
77. Mason E, McKinlay A, Clark I. Cooling rate effects in thermoluminescence dosimetry grade lithium fluoride. Implications for practical dosimetry. *Phys Med Biol*. 1976;21:60–66.
78. Pedersen K, Andersen TD, Rodal J, Olsen DR. Sensitivity and stability of LiF thermoluminescence dosimeters. *Med Dosim*. 1995;20:263–267.
79. Umisedo NK, Yoshimura EM, Gasparian PBR, Yukihara EG. Comparison between blue and green stimulated luminescence of Al2O3:C. *Radiat Meas*. 2010;45:151–156.
80. Yukihara EG, Gaza R, McKeever SW, Soares CG. Optically stimulated luminescence and thermoluminescence efficiencies for high-energy heavy charged particle irradiation in Al2O3:C. *Radiat Meas*. 2004;38:59–70.
81. ICRP Publication 103. The 2007 recommendations of the international commission on radiological protection. ICRP; 2007.
82. Kron T. Thermoluminescence dosimetry and its applications in medicine–Part 1: physics, materials and equipment. *Australas Phys Eng Sci Med*. 1994;17:175–199.
83. Thomas SJ, Palmer N. The use of carbon-loaded thermoluminescent dosimeters for the measurement of surface doses in megavoltage X-ray-beams. *Med Phys*. 1989;16:902–904.
84. Perera F, Chisela F, Stitt L, Engel J, Venkatesan V. TLD skin dose measurements and acute and late effects after lumpectomy and high-dose-rate brachytherapy only for early breast cancer. *Int J Radiat Oncol*. 2005;62:1283–1290.
85. Kron T, Butson M, Hunt F, Denham J. TLD extrapolation for skin dose determination in vivo. *Radiother Oncol*. 1996;41:119–123.
86. Lin JP, Chu TC, Lin SY, Liu MT. Skin dose measurement by using ultra-thin TLDs. *Appl Radiat Isotopes*. 2001;55:383–391.
87. Kry SF, Olch A, Mohan R. Comment on "Monte Carlo evaluations of the absorbed dose and quality dependence of Al2O3 in radiotherapy photon beams" [Med. Phys. 36(10), 4421–4424 (2009)]. *Med Phys*. 2015;42:2648–2649.
88. Devic S, Seuntjens J, Abdel-Rahman W, et al. Accurate skin dose measurements using radiochromic film in clinical applications. *Med Phys*. 2006;33:1116–1124.
89. Li XA, Soubra M, Szanto J, Gerig LH. Lateral electron equilibrium and electron contamination in measurements of head-scatter factors using miniphantoms and brass caps. *Med Phys*. 1995;22:1167–1170.
90. Kron T, Ostwald PM, Hamilton CS, Denham JW. TLD extrapolation measurements for entrance and exit dose in radiotherapy. *Radiat Prot Dosim*. 1996;66:323–326.
91. Nilsson B, Sorcini B. Surface dose measurements in clinical photon beams. *Acta Oncol*. 1989;28:537–542.
92. Azangwe G, Grochowska P, Georg D et al. Detector to detector corrections: a comprehensive experimental study of detector specific correction factors for beam output measurements for small radiotherapy beams, *Med Phys*. 2014;41:072103.
93. Duggan DM, Coffey CW 2nd. Small photon field dosimetry for stereotactic radiosurgery. *Med Dosim*. 1998;23:153–159.
94. Heydarian M, Hoban PW, Beddoe AH. A comparison of dosimetry techniques in stereotactic radiosurgery. *Phys Med Biol*. 1996;41:93–110.
95. Schell MC, Bova FJ, Larson DA, et al. AAPM report No. 54: stereotactic radiosurgery. American Association of Physicists in Medicine; 1995.

96. Benmakhlouf H, Johansson J, Paddick I, Andreo P. Monte Carlo calculated and experimentally determined output correction factors for small field detectors in Leksell Gamma Knife Perfexion beams. *Phys Med Biol*. 2015;60:3959–3973.
97. Zoros E, Moutsatsos A, Pappas EP, et al. Monte Carlo and experimental determination of correction factors for gamma knife perfexion small field dosimetry measurements. *Phys Med Biol*. 2017;62:7532–7555.
98. Moignier C, Huet C, Barraux V, et al. Determination of small field output factors and correction factors using a Monte Carlo method for a 1000 MU/min CyberKnife (R) system equipped with fixed collimators. *Radiat Meas*. 2014;71:287–292.
99. Fan CJ, Devanna WG, Leybovich LB, et al. Dosimetry of very-small (5–10 mm) and small (12.5-40 mm) diameter cones and dose verification for radiosurgery with 6-MV X-ray beams. *Stereotact Funct Neurosurg*. 1996;67:183–197.
100. Friedman WA, Bova FJ. The University of Florida radiosurgery system. *Surg Neurol*. 1989;32:334–342.
101. Serago CF, Houdek PV, Hartmann GH, Saini DS, Serago ME, Kaydee A. Tissue maximum ratios (and other parameters) of small circular 4, 6, 10, 15 and 24 MV x-ray beams for radiosurgery. *Phys Med Biol*. 1992;37:1943–1956.
102. Bucciolini M, Russo S, Banci Buonamici F, Pini S, Silli P. Dosimetric characterization of a bi-directional micromultileaf collimator for stereotactic applications. *Med Phys*. 2002;29:1456–1463.
103. Cosgrove VP, Jahn U, Pfaender M, Bauer S, Budach V, Wurm RE. Commissioning of a micro multi-leaf collimator and planning system for stereotactic radiosurgery. *Radiother Oncol*. 1999;50:325–336.
104. Wu A, Lindner G, Maitz AH, et al. Physics of gamma knife approach on convergent beams in stereotactic radiosurgery. *Int J Radiat Oncol Biol Phys*. 1990;18:941–949.
105. Yu C, Jozsef G, Apuzzo ML, Petrovich Z. Measurements of the relative output factors for cyberknife collimators. *Neurosurgery.* 2004;54:157–162.
106. Yu C, Luxton G, Apuzzo ML, Petrovich Z. TLD measurements of the relative output factors for the Leksell Gamma Knife. *Stereotact Funct Neurosurg*. 1999;72:150–158.
107. Ibbott GS, Followill DS, Molineu HA, Lowenstein JR, Alvarez PE, Roll JE. Challenges in credentialing institutions and participants in advanced technology multi-institutional clinical trials. *Int J Radiat Oncol Biol Phys*. 2008;71:S71–S75.
108. Pham C. University of Texas MD Anderson Cancer Center, 2013.
109. Charles PH, Crowe SB, Kairn T, et al. The effect of very small air gaps on small field dosimetry. *Phys Med Biol*. 2012;57:6947–6960.
110. Ahmed MF, Eller SA, Schnell E, et al. Development of a 2D dosimetry system based on the optically stimulated luminescence of Al2O3. *Radiat Meas*. 2014;71:187–192.
111. Ahmed MF, Shrestha N, Schnell E, Ahmad S, Akselrod MS, Yukihara EG. Characterization of Al2O3 optically stimulated luminescence films for 2D dosimetry using a 6 MV photon beam. *Phys Med Biol*. 2016;61:7551–7570.
112. Estar-database. National Institute of Standards and Technology: estar stopping-power and range tables for electrons. http://physics.nist.gov/PhysRefData/Star/Text/ESTAR.html.
113. Robar V, Zankowski C, Pla MO, Podgorsak EB. Thermoluminescent dosimetry in electron beams: energy dependence. *Med Phys*. 1996;23:667–673.
114. Karzmark CJ, Anderson J, Buffa A, et al. AAPM report No. 23; Total skin electron therapy: technique and dosimetry. American Association of Physicists in Medicine. 1987.
115. Lawless MJ, Junell S, Hammer C, DeWerd LA. Response of TLD-100 in mixed fields of photons and electrons. *Med Phys*. 2013;40:012103.
116. Sawakuchi GO, Yukihara EG. Analytical modeling of relative luminescence efficiency of Al2O3: C optically stimulated luminescence detectors exposed to high-energy heavy charged particles. *Phys Med Biol*. 2012;57:437–454.
117. Sawakuchi GO, Yukihara EG, McKeever SWS, Benton ER. Optically stimulated luminescence fluence response of Al2O3: C dosimeters exposed to different types of radiation. *Radiat Meas*. 2008;43:450–454.
118. Carlsson CA, Carlsson GA. Proton dosimetry: measurement of depth doses from 185-MeV protons by means of thermoluminescent LiF. *Radiat Res*. 1970;42:207–219.
119. Kerns JR, Kry SF, Sahoo N. Characteristics of optically stimulated luminescence dosimeters in the spread-out Bragg peak region of clinical proton beams. *Med Phys*. 2012;39:1854–1863.
120. Sawakuchi GO, Yukihara EG, McKeever SWS, et al. Relative optically stimulated luminescence and thermoluminescence efficiencies of Al2O3: C dosimeters to heavy charged particles with energies relevant to space and radiotherapy dosimetry. *J Appl Phys*. 2008;104:124903.
121. Yukihara EG, Doull BA, Ahmed M, et al. Time-resolved optically stimulated luminescence of Al2O3: C for ion beam therapy dosimetry. *Phys Med Biol*. 2015;60:6613–6638.
122. Berger T, Hajek M. On the linearity of the high-temperature emission from (LiF)-Li-7:Mg, Ti (TLD-700). *Radiat Meas*. 2008;43:1467–1473.
123. Guan F, Geng C, Carlson DJ, et al. Amechanistic relative biological effectiveness model-based biological dose optimization for charged particle radiobiology studies. *Phys Med Biol*. 2019;64:015008.
124. Edmund JM, Andersen CE, Greilich S. A track structure model of optically stimulated luminescence from Al2O3: C irradiated with 10–60 MeV protons. *Nucl Instrum Meth B*. 2007;262:261–275.
125. Busuoli G, Cavallini A, Fasso A, Rimondi O. Mixed radiation dosimetry with Lif (Tld-100). *Phys Med Biol*. 1970;15:673–681.
126. Schoner W, Vana N, Fugger M. The LET dependence of LiF : Mg, Ti dosemeters and its application for LET measurements in mixed radiation fields. *Radiat Prot Dosimetry.* 1999;85:263–266.
127. Loncol T, Hamal M, Denis JM, Vynckier S, Wambersie A, Scalliet P. Response analysis of TLD-300 dosimeters in heavy-particle beams. *Phys Med Biol*. 1996;41:1665–1678.
128. Harvey JA, Thomas EM, Kearfott KJ. Quantification of various factors influencing the precision of thermoluminescent detector calibrations for new and used chip sets. *Health Phys*. 2011;100:S79–S91.
129. DeWerd LA, Ibbott GS, Meigooni AS, et al. A dosimetric uncertainty analysis for photon-emitting brachytherapy sources: report of AAPM Task Group No. 138 and GEC-ESTRO. *Med Phys*. 2011;38:782–801.
130. Das R, Toye W, Kron T, Williams S, Duchesne G. Thermoluminescence dosimetry for in-vivo verification of high dose rate brachytherapy for prostate cancer. *Australas Phys Eng Sci Med*. 2007;30:178–184.
131. Kapp KS, Stuecklschweiger GF, Kapp DS, Hackl AG. Dosimetry of intracavitary placements for uterine and cervical-carcinoma - results of orthogonal film, Tld, and Ct-assisted techniques. *Radiother Oncol*. 1992;24:137–146.
132. Toye W, Das R, Kron T, Franich R, Johnston P, Duchesne G. An in vivo investigative protocol for HDR prostate brachytherapy using urethral and rectal thermoluminescence dosimetry. *Radiother Oncol*. 2009;91:243–248.
133. Raffi JA, Davis SD, Hammer CG, et al. Determination of exit skin dose for Ir-192 intracavitary accelerated partial breast irradiation with thermoluminescent dosimeters. *Med Phys*. 2010;37:2693–2702.
134. Taylor REP, Rogers DWO. EGSnrc Monte Carlo calculated dosimetry parameters for (192)Ir and (169)Yb brachytherapy sources. *Med Phys*. 2008;35:4933–4944.
135. Rivard MJ, Ballester F, Butler WM, et al. Supplement 2 for the 2004 update of the AAPM Task Group No. 43 Report: joint recommendations by the AAPM and GEC-ESTRO. *Med Phys*. 2017;44:E297–E338.
136. Meigooni AS, Meli JA, Nath R. Influence of the variation of energy-spectra with depth in the dosimetry of Ir-192 using Lif Tld. *Phys Med Biol*. 1988;33:1159–1170.
137. Tedgren AC, Elia R, Hedtjarn H, Olsson S, Carlsson GA. Determination of absorbed dose to water around a clinical HDR Ir-192 source using LiF:Mg, Ti TLDs demonstrates an LET dependence of detector response. *Med Phys*. 2012;39:1133–1140.
138. Karaiskos P, Angelopoulos A, Sakelliou L, et al. Monte Carlo and TLD dosimetry of an Ir-192 high dose-rate brachytherapy source. *Med Phys*. 1998;25:1975–1984.
139. Reed JL, Rasmussen BE, Davis SD, Micka JA, Culberson WS, DeWerd LA. Determination of the intrinsic energy dependence of LiF:Mg, Ti thermoluminescent dosimeters for I-125 and Pd-103 brachytherapy sources relative to Co-60. *Med Phys*. 2014;41:122103.
140. Kennedy RM, Davis SD, Micka JA, DeWerd LA. Experimental and Monte Carlo determination of the TG-43 dosimetric parameters for the model 9011 THINSeed (TM) brachytherapy source. *Med Phys*. 2010;37:1681–1688.

141. Muench PJ, Meigooni AS, Nath R, Mclaughlin WL. Photon energy-dependence of the sensitivity of radiochromic film and comparison with silver-halide film and lif tlds used for brachytherapy dosimetry. *Med Phys*. 1991;18:769–775.
142. Perez-Calatayud J, Granero D, Ballester F. Phantom size in brachytherapy source dosimetric studies. *Med Phys*. 2004;31:2075–2081.
143. Tedgren AC, Carlsson GA. Influence of phantom material and dimensions on experimental (192)Ir dosimetry. *Med Phys*. 2009;36:2228–2235.
144. DeWerd LA, Liang Q, Reed JL, Culberson WS. The use of TLDs for brachytherapy dosimetry. *Radiat Meas*. 2014;71:276–281.
145. Rodriguez M, Rogers DWO. Effect of improved TLD dosimetry on the determination of dose rate constants for I-125 and Pd-103 brachytherapy seeds. *Med Phys*. 2014;41:114301.
146. Holmes SM, DeWerd LA, Micka JA. Experimental determination of the radial dose function of Sr-90/Y-90 IVBT sources. *Med Phys*. 2006;33:3225–3233.
147. Casey KE, Alvarez P, Kry SF, Howell RM, Lawyer A, Followill D. Development and implementation of a remote audit tool for high dose rate (HDR) Ir-192 brachytherapy using optically stimulated luminescence dosimetry. *Med Phys*. 2013;40:112102.
148. Tien CJ, Ebeling R 3rd, Hiatt JR, Curran B, Sternick E. Optically stimulated luminescent dosimetry for high dose rate brachytherapy. *Front Oncol*. 2012;2:91.
149. Haworth A, Butler DJ, Wilfert L, et al. Comparison of TLD calibration methods for 192Ir dosimetry. *J Appl Clin Med Phys*. 2013;14:4037.
150. Lavoie L, Ghita M, Brateman L, Arreola M. Characterization of a commercially-available, optically-stimulated luminescent dosimetry system for use in computed tomography. *Health Phys*. 2011;101:299–310.
151. Brunner CC, Stern SH, Minniti R, Parry MI, Skopec M, Chakrabarti K. CT head-scan dosimetry in an anthropomorphic phantom and associated measurement of ACR accreditation-phantom imaging metrics under clinically representative scan conditions. *Med Phys*. 2013; 40:081917.
152. Giaddui T, Cui Y, Galvin J, Yu Y, Xiao Y. Comparative dose evaluations between XVI and OBI cone beam CT systems using Gafchromic XRQA2 film and nanoDot optical stimulated luminescence dosimeters. *Med Phys*. 2013;40:062102.
153. Ding GX, Malcolm AW. An optically stimulated luminescence dosimeter for measuring patient exposure from imaging guidance procedures. *Phys Med Biol*. 2013;58:5885–5897.
154. Vrieze TJ, Sturchio GM, McCollough CH. Technical note: precision and accuracy of a commercially available CT optically stimulated luminescent dosimetry system for the measurement of CT dose index. *Med Phys*. 2012;39:6580–6584.
155. Dewerd LA, Chiu NB. The determination of radiation-dose by mail for diagnostic radiological examinations with thermoluminescent dosimeters. *Radiat Prot Dosimetry.* 1993;47:509–512.
156. Nawfel RD, Judy PF, Silverman SG, Hooton S, Tuncali K, Adams DF. Patient and personnel exposure during CT fluoroscopy-guided interventional procedures. *Radiology.* 2000;216:180–184.
157. Buls N, Pages J, de Mey J, Osteaux M. Evaluation of patient and staff doses during various CT fluoroscopy guided interventions. *Health Phys*. 2003;85:165–173.
158. Vano E. ICRP recommendations on 'managing patient dose in digital radiology'. *Radiat Prot Dosimetry.* 2005;114:126–130.
159. Sanchez RM, Vano E, Fernandez JM, Escaned J. Evaluation of a real-time display for skin dose map in cardiac catheterisation procedures. *Radiat Prot Dosimetry.* 2015;165:240–243.
160. Jibiri NN, Olowookere CJ. Evaluation of dose-area product of common radiographic examinations towards establishing a preliminary diagnostic reference levels (PDRLs) in Southwestern Nigeria. *J Appl Clin Med Phys*. 2016;17:392–404.
161. Scarboro S, Cody D, Stingo F, et al. Calibration strategies for the use of the nanoDot OLSD in CT applications. *J Appl Clin Med Phys.* 2019;20 (1):331–339
162. Davis SD, Ross CK, Mobit PN, Van der Zwan L, Chase WJ, Shortt KR. The response of lif thermoluminescence dosemeters to photon beams in the energy range from 30 kV x rays to 60Co gamma rays. *Radiat Prot Dosimetry.* 2003;106:33–43.
163. Yukihara EG, Ruan C, Gasparian PB, Clouse WJ, Kalavagunta C, Ahmad S. An optically stimulated luminescence system to measure dose profiles in x-ray computed tomography. *Phys Med Biol*. 2009;54:6337–6352.
164. Aznar MC, Medin J, Hemdal B, et al. A Monte Carlo study of the energy dependence of Al2O3: C crystals for real-time in vivo dosimetry in mammography. *Radiat Prot Dosimetry.* 2005;114:444–449.
165. Mobit P, Agyingi E, Sandison G. Comparison of the energy-response factor of LiF and Al2O3 in radiotherapy beams. *Radiat Prot Dosimetry.* 2006;119:497–499.
166. Ruan C, Yukihara EG, Clouse WJ, Gasparian PB, Ahmad S. Determination of multislice computed tomography dose index (CTDI) using optically stimulated luminescence technology. *Med Phys*. 2010;37:3560–3568.
167. Konnai A, Nariyama N, Ohnishi S, Odano N. Energy response of LiF and Mg2SiO4 TLDs to 10–150 keV monoenergetic photons. *Radiat Prot Dosimetry.* 2005;115:334–336.
168. Knezevic Z, Stolarczyk L, Bessieres I, Bordy JM, Miljanic S, Olko P. Photon dosimetry methods outside the target volume in radiation therapy: optically stimulated luminescence (OSL), thermoluminescence (TL) and radiophotoluminescence (RPL) dosimetry. *Radiat Meas*. 2013;57:9–18.
169. Kry SF, Titt U, Followill D, et al. A Monte Carlo model for out-of-field dose calculation from high-energy photon therapy. *Med Phys*. 2007;34:3489–3499.
170. Kry SF, Titt U, Ponisch F, et al. A Monte Carlo model for calculating out-of-field dose from a Varian 6 MV beam. *Med Phys*. 2006;33:4405–4413.
171. Starkschall G, Stgeorge FJ, Zellmer DL. Surface dose for megavoltage photon beams outside the treatment field. *Med Phys*. 1983;10:906–910.
172. Kry SF, Price M, Followill D, Mourtada F, Salehpour M. The use of LiF (TLD-100) as an out-of-field dosimeter. *J Appl Clin Med Phys*. 2007;8:2679.
173. Klemic GA, Azziz N, Marino SA. The neutron response of Al2O3:C, (LiF)-Li-7:Mg, Cu, P, and (LiF)-Li-7:Mg, Ti TLDs. *Radiat Prot Dosim*. 1996;65:221–226.
174. Attix FH. *Introduction to Radiological Physics and Radiation Dosimetry.* New York: Wiley; 1986.
175. Mendez R, Iniguez MP, Barquero R, et al. Response components of LiF : Mg, Ti around a moderated Am-Be neutron source. *Radiat Prot Dosim*. 2002;98:173–178.
176. Howell RM, Burgett EA, Hertell NE, Kry SF, Wang Z, Salehpour M. Measurement of high-energy neutron spectra with a Bonner Sphere Extension System. *Nucl Technol*. 2009;168:333–339.
177. Howell RM, Burgett EA. Secondary neutron spectrum from 250-MeV passively scattered proton therapy: measurement with an extended-range Bonner sphere system. *Med Phys*. 2014;41:092104.
178. Howell RM, Ferenci MS, Hertel NE, Fullerton GD. Investigation of secondary neutron dose for 18 MV dynamic MLC IMRT delivery. *Med Phys*. 2005;32:786–793.
179. Howell RM, Kry SF, Burgett E, Hertel NE, Followill DS. Secondary neutron spectra from modern Varian, Siemens, and Elekta linacs with multileaf collimators. *Med Phys*. 2009;36:4027–4038.
180. Reft CS, Runkel-Muller R, Myrianthopoulos L. In vivo and phantom measurements of the secondary photon and neutron doses for prostate patients undergoing 18 MV IMRT. *Med Phys*. 2006;33:3734–3742.
181. Howell RM, Burgett EA, Wiegel B, Hertel NE. Calibration of a Bonner sphere extension (BSE) for high-energy neutron spectrometry. *Radiat Meas*. 2010;45:1233–1237.
182. Kry SF, Howell RM, Salehpour M, Followill DS. Neutron spectra and dose equivalents calculated in tissue for high-energy radiation therapy. *Med Phys*. 2009;36:1244–1250.
183. Perks CA, Le Roy G, Prugnaud B. Introduction of the InLight monitoring service. *Radiat Prot Dosimetry.* 2007;125:220–223.
184. Yukihara EG, Mittani JC, Vanhavere F, Akselrod MS. Development of new optically stimulated luminescence (OSL) neutron dosimeters. *Radiat Meas*. 2008;43:309–314.
185. Rutala WA, Weber DJ. Disinfection and sterilization in health care facilities: what clinicians need to know. *Clin Infect Dis*. 2004;39:702–709.

186. Budanec M, Knezevic Z, Bokulic T, et al. Comparison of doses calculated by the Monte Carlo method and measured by Lif TLD in the buildup region for a Co-60 photon beam. *Appl Radiat Isotopes*. 2008;66:1925–1929.
187. Kron T, Elliot A, Wong T, Showell G, Clubb B, Metcalfe P. X-ray surface dose measurements using Tld extrapolation. *Med Phys*. 1993;20:703–711.
188. Das A, Dhara S, Patnaik A. Electron transport across fractal-like nanocrystalline clusters in N+ ion-beam induced poly(phenylene oxide). *J Chem Phys*. 2001;114:8573–8582.
189. Pradhan AS, Gopalakrishnan AK, Iyer PS. Dose measurement at high atomic number interfaces in megavoltage photon beams using TLDs. *Med Phys*. 1992;19:355–356.
190. Verhaegen F. Evaluation of the EGSnrc Monte Carlo code for interface dosimetry near high-Z media exposed to kilovolt and Co-60 photons. *Phys Med Biol*. 2002;47:1691–1705.
191. Kron T, DeWerd L, Mobit P, et al. A checklist for reporting of thermoluminescence dosimetry (TLD) measurements. *Phys Med Biol*. 1999;44: L15–L17.